PLOS Biology

RESEARCH ARTICLE

Regulation of working memory switches from striatal dopamine D2-receptor to D1-receptor neurons under high cognitive load

Xing-jun Chen[1], Fei Li[1], Xinyue Zhao[1], Long Chen[1], Jin Xue[1], Zhimo Yao[1], Zuobin Gan[1], Xiaoyue Lian[1], Zhenghao Liu[1], Luyao Tong[1], Qingshan Yan[1], Linan Qiu[1,2], Qin Wang[1], Jiang-fan Chen[1,2☯*], Zhihui Li[1,2☯*]

1 The Molecular Neuropharmacology Laboratory and the Eye-Brain Research Center, The State Key Laboratory of Ophthalmology, Optometry and Vision Science, School of Ophthalmology & Optometry and Eye Hospital, Wenzhou Medical University, Wenzhou, China, **2** Oujiang Laboratory (Zhejiang Lab for Regenerative Medicine, Vision and Brain Health), School of Ophthalmology & Optometry and Eye Hospital, Wenzhou Medical University, Wenzhou, China

☯ These authors contributed equally to this work.
* chenjf555@gmail.com (J-fC); smart_dream@wmu.edu.cn (ZL)

Check for updates

OPEN ACCESS

Citation: Chen X-j, Li F, Zhao X, Chen L, Xue J, Yao Z, et al. (2025) Regulation of working memory switches from striatal dopamine D2-receptor to D1-receptor neurons under high cognitive load. PLoS Biol 23(7): e3003289. https://doi.org/10.1371/journal.pbio.3003289

Academic Editor: Jones Parker, Northwestern University Feinberg School of Medicine, UNITED STATES OF AMERICA

Received: December 15, 2024

Accepted: July 2, 2025

Published: July 24, 2025

Copyright: © 2025 Chen et al. This is an open access article distributed under the terms of the Creative Commons Attribution License, which permits unrestricted use, distribution, and reproduction in any medium, provided the original author and source are credited.

Data availability statement: All relevant data are within the paper and its Supporting information files.

Funding: This study was supported by the National Key Research and Development Program of China (No. 2022YFE0210100 to

Abstract

Working memory (WM) is a fundamental cognitive function crucial adaptive behavior. The intricate interplay between the frontal cortex and striatum in governing WM maintenance and updating remains a central question. In this study, we employed optogenetics to demonstrate that inhibiting both dorsomedial striatum (DMS) D_1R- and D_2R-neurons enhances WM, while their activation impairs it across T-maze and operant-based delayed-non-match-to-place (DNMTP) paradigms in mice. Notably, these neurons selectively modulate WM maintenance and retrieval, with no impact on encoding. Analysis through signal detection theory (SDT) revealed specific regulation of WM signal detection sensitivity, with no alterations in motivational or motor states during the operant DNMTP task. Interestingly, DMS D_2R-neurons govern WM regulation under low cognitive load, switching to D_1R-neurons as cognitive load increases. Activation of DMS D_1R-neurons during the delay phase severely impairs WM under high cognitive load, a deficit rescued by optogenetic inhibition of dopaminergic neurons in the ventral tegmental area (VTA) and substantia nigra pars compacta (SNc), or dopaminergic terminals in DMS. Additionally, treatment with the D_1R antagonist SCH39166, but not the D_2R antagonist Sulpiride mitigates these impairments. Collectively, our findings propose a "relay" model wherein cognitive load-dependent WM control switches from DMS D_2R- to D_1R-neurons, offering nuanced, complementary, and inhibitory regulation of WM maintenance and retrieval. This study suggests potential strategies to enhance WM by promoting a suppressive state in DMS and to increase WM capacity through specific modulation of DMS D_1R-neurons.

J.F.C. and Z.L., https://www.cstec.org.cn/), the National Natural Science Foundation of China (No. 81971031 to Z.L., https://www.nsfc.gov.cn/), the Key Program of the Zhejiang Provincial Natural Science Foundation (No. ZCLZ25H2501 to Z.L., https://zjnsf.kjt.zj.gov.cn/), the National Natural Science Foundation of China (Original Exploration Project) (No. 82151308 to J.F.C., https://www.nsfc.gov.cn/), the National Natural Science Foundation of China, Research Fund for International Senior Scientists (No. 82150710558 to J.F.C., https://www.nsfc.gov.cn/), the Science & Technology Initiative STI2030-Major Projects (No.2021ZD0203400 to J.F.C., https://www.cncbd.org.cn/), the Key Research and Development Program of Zhejiang Province (No. 2023C03079 to J.F.C., https://kjt.zj.gov.cn/), the Scientific Research Starting Foundation of Oujiang Laboratory (Zhejiang Lab for Regenerative Medicine, Vision and Brain Health) (No.OJQDSP2022007 to J.F.C., https://www.ojlab.cn/), the Project of State Key Laboratory of Ophthalmology, Optometry and Visual Science, Wenzhou Medical University (No. J01-20190101 to J.F.C., https://www.wzeye.cn/), the Scientific Research Starting Foundation of Wenzhou Medical University (No. QTJ12003 to J.F.C., https://www.wmu.edu.cn/), the Laboratory Construction Funding from the Department of Science and Technology of Zhejiang Province (No. 2023ZY1011 to J.F.C., https://www.wzeye.cn/). The funders had no role in study design, data collection and analysis, decision to publish, or preparation of the manuscript.

Competing interests: The authors have declared that no competing interests exist.

Abbreviations : CNO, clozapine-n-oxide; DIO, double-inverted orientation; DNMTP, delayed-non-match-to-place; DMS, dorsomedial striatum; GPe, globus pallidus; i.p., intraperitoneally; MSNs, medium spiny neurons; mTH, mouse tyrosine hydroxylase; NMTP, non-matching to place; PFC, parietal and prefrontal cortex; RI, responsivity index; SDT, signal detection theory; SI, sensitivity index; SNc, substantia nigra pars compacta; SNR, substantia nigra pars reticulate; VTA, ventral tegmental area; WM, working memory.

Introduction

Working memory (WM) is a capacity-limited, short-term storage system crucial for preserving, manipulating, and updating information to support adaptive behaviors [1]. Aging and neuropsychiatric disorders such as Alzheimer's disease and schizophrenia are characterized by significant deficits in WM [2–4]. A distributed WM network, featuring functional specialization across sensory cortex, the parietal and prefrontal cortex (PFC), as well as subcortical structures, is essential for information storage and processing within WM [5–8].

The PFC plays a central role in WM maintenance, while the dorsomedial striatum (DMS) within the basal ganglia (BG) is integral for WM updating. Various imaging, metabolic, and electrophysiological studies have demonstrated increased activity in the caudate of humans and primates during WM tasks [9–11]. Specifically, sequential activity in DMS have been documented spanning the entire delay period and was dissociated from stimulus encoding activity in WM [12]. Moreover, the stimulus preceding activities in both the PFC and BG were associated with the filtering of irrelevant information and variations in WM capacity [13]. Disruptions in WM have been observed following electric stimulation [14] or caudate lesions [15,16]. Imaging and computational modeling studies suggest that the striatum functions as a gatekeeper, selecting behaviorally relevant information for WM ("input" gating) and choosing contextual representations in the PFC to drive responses ("output" gating), thereby enabling balanced cognitive control with both flexibility and stability through corticostriatal interactions [17–19].

The DMS modulates behavior via two types of neurons: medium spiny neurons (MSNs) expressing dopamine D1 receptor (D_1R-neurons) that project directly to the substantia nigra pars reticulata (SNR), and MSNs expressing dopamine D2 receptor-expressing (D_2R-neurons) that project to the external segment of the globus pallidus (GPe) and subsequently to the SNR via the subthalamic nucleus [20,21]. These neurons function antagonistically in motor control and reward-based behaviors [22,23], but recent studies suggest more complex controls in motor learning, action selection, and reinforcement learning [24–30]. Despite the DMS's critical involvement in WM, the specific involvement of DMS D_1R- and D_2R-neurons in distinct WM information processing and capacity control remain poorly understood, primarily due to the lack of targeted manipulation methods with sufficient WM-required temporal resolution.

This study addresses three key questions regarding the DMS control of WM. First, we investigate whether DMS D_1R- and D_2R-neurons operate antagonistically or cooperatively in WM control, and identify the specific phase(s) of information processing-encoding, maintenance, or retrieval-they selectively influence. Second, we access whether DMS D_1R- and D_2R-neurons differentially engage in WM tasks that involve varying cognitive loads. Lastly, we examine how DMS dopamine signaling causally modulates WM.

Our analyses, utilizing optogenetic and chemogenetic manipulations targeted specifically at DMS D_1R- and D_2R-neurons, combined with T-maze- and operant-based delayed-non-match-to-place (DNMTP) WM paradigms, reveal that the DMS D_1R- and

D_2R-neurons exert coordinated and inhibitory control over WM maintenance and retrieval. Notably, we identify a novel "relay" mechanism, indicating that the DMS regulation of WM switches from D_2R- to D_1R-neurons in response to increased cognitive load. Activation of DMS D_1R-neurons during the delay phase severely impairs WM under high cognitive load, a deficit rescued by optogenetic inhibition of dopaminergic neurons in the ventral tegmental area (VTA) and substantia nigra pars compacta (SNc), or dopaminergic terminals in DMS. Additionally, treatment with the D1R antagonist SCH39166, but not the D2R antagonist Sulpiride mitigates these impairments. This research offers a cellular mechanism wherein these two DMS neurons types collaborate to confer continuous and complementary control of WM. It builds on previous models of BG function, moving beyond classic "go/no-go" [31,32], "complementary" [24,25], and "competitive" [33] frameworks in procedural learning (motor skills and habits) [34], to introduce a "relay" control model for declarative learning (WM) [35,36].

Results

Optogenetic inhibition of DMS D_2R-neurons selectively promoted WM maintenance and retrieval under low cognitive load in the T-maze DNMTP task

The T-maze DNMTP task, in which each trial consists of "sample", "delay", and "choice" phases (Materials and methods), facilitates assessment of WM encoding, maintenance, and retrieval respectively [37–41]. To elucidate the roles of DMS D_2R-neurons in these distinct WM processes, we optogenetically inhibited these neurons individually during specific phases of the task. Moreover, WM load can be assessed through manipulating item capacity or maintenance duration. In animal models, where item capacity manipulations are challenging, delay duration is used as an alternative method to modulate WM load. Longer delays increase cognitive load, as neural representations must be actively maintained against decay or interference for extended periods [42–47]. As the DNMTP task allows for adjustments in task difficulty through varying the length of the "delay" period [48], we also investigated whether D_2R-neurons exhibit load-dependent modulation as the temporal demands of WM maintenance change. During task acquisition, a shorter delay (10 s) was introduced, representing low cognitive load. Subsequently, we increased the delay to 20, 30, and 60 s, which resulted in decreased WM performance, indicating higher cognitive load.

The Cre-dependent ArchT-GFP or GFP AAVs were expressed in DMS of Adora2a-Cre mice, and the proper targeting of D_2R-neurons was verified through their projection to GPe (Fig 1A). Quantitative analysis revealed significant induction of c-Fos expression, primarily in ArchT-GFP$^-$-expressing cells (Figs 1B, 1C and S1A), which stems from the striatum's highly complex microcircuitry where MSNs form extensive inhibitory connections not only with downstream targets but also with each other through lateral inhibition networks [49–51]. With 3 separate sets of animals, we delivered 560 nm laser to DMS of Adora2a-Cre mice expressing either ArchT-GFP or GFP in D_2R-neurons at specific phases of the task. Inhibition of DMS D_2R-neurons during the "sample" phase showed no notable effect on WM performance neither under low nor high cognitive loads (Fig 1D–1F); however, inhibiting DMS D_2R-neurons during the "delay" (Fig 1G and 1H) or "choice" phases (Fig 1J and 1K) significantly enhanced WM performance under low cognitive load. In contrast, under higher cognitive loads, optogenetic inhibition of DMS D_2R-neurons during the "delay" and "choice" phases had no significant impact on WM performance (Fig 1I for "delay" light stimulation, Fig 1L for "choice" light stimulation). Moreover, ArchT silencing of D_2R-neurons did not affect locomotion, ruling out its potential confounding effects (S2A Fig). These findings highlight the critical roles of DMS D_2R-neurons in WM maintenance and retrieval specifically under low cognitive load, while their involvement in encoding the sample location appears minimal.

Optogenetic activation of anterior but not posterior DMS D_2R-neurons impaired WM under low cognitive load in the T-maze DNMTP task

Next, we investigated the effects of optogenetically activation of D_2R-neurons on WM performance. We expressed Cre-dependent ChR2-mCherry or mCherry AAVs in DMS of Adora2a-Cre mice (Fig 2A, AP: +0.98 mm). Stimulation of ChR2

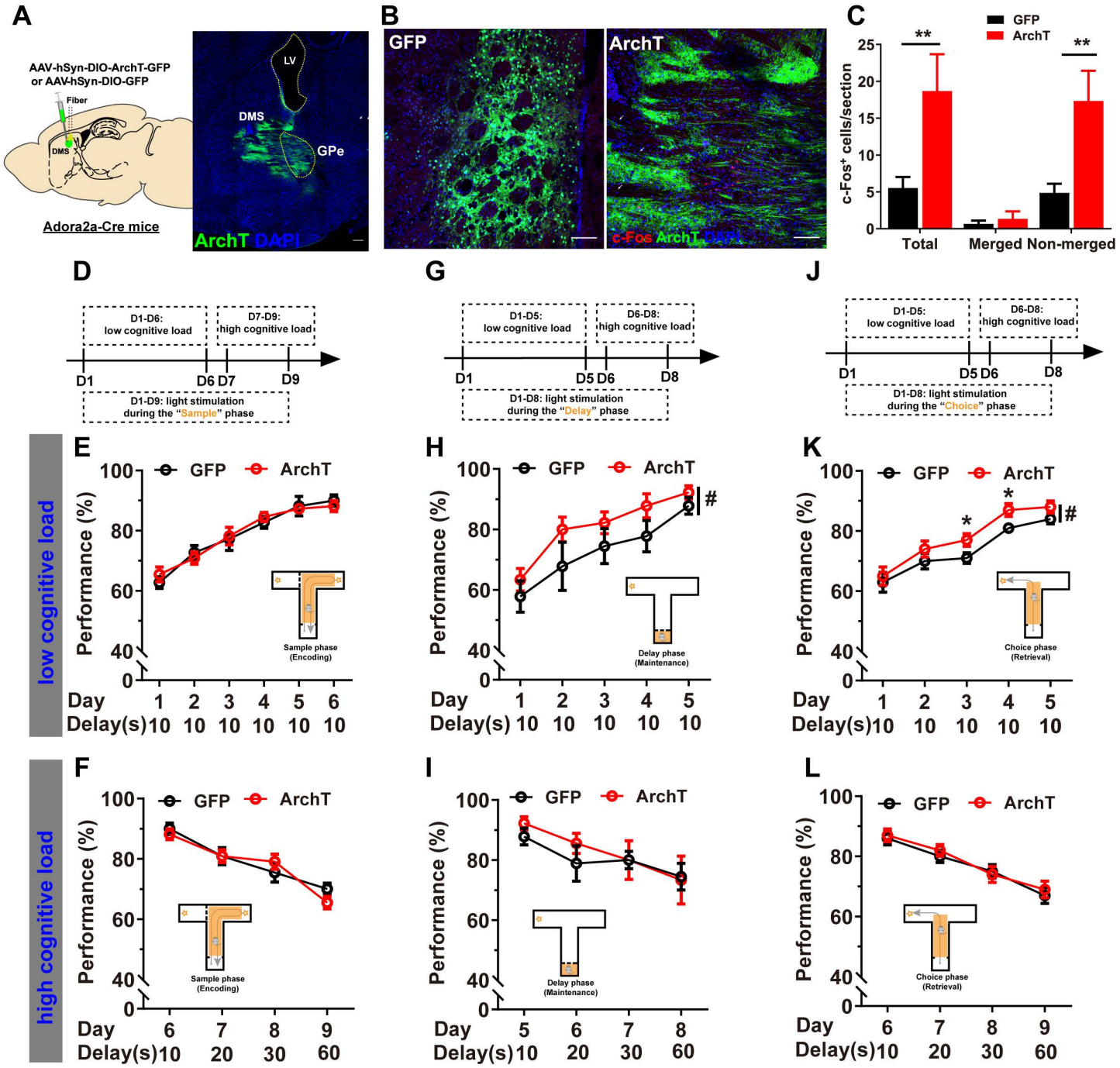

Fig 1. Optogenetic inhibition of D_2R-neurons selectively promoted WM maintenance and retrieval under low cognitive load. A Left: Schematic representation of virus injection and optic fiber implantation in DMS of Adora2a-Cre (+) mice. Right: Representative images showing ArchT (green) and DAPI (blue) in DMS, as well as projections to GPe in green. Scale bar, 100 μm. **B** Representative images of c-Fos induction following optogenetic inhibition of DMS D_2R-neurons. **C** Quantitative analysis revealed a significant increase in c-Fos expression following photoinhibition of D_2R-neurons, primarily non-merged with the virus (Independent-Sample *t* test, $^{**}p < 0.01$). **D** Schematic of the experimental design for light stimulation during the "sample" phase. Photoinhibition of DMS D_2R-neurons during the "sample" phase did not significantly affect WM under both low (**E**) and high cognitive loads (**F**, repeated measures [RM] two-way ANOVA, ns $P > 0.05$; $n = 11$ for both groups). **G** Schematic of the experimental design for light stimulation during the "delay" phase. Photoinhibition of DMS D_2R-neurons during the 10 s "delay" phase resulted in a significant improvement in WM performance under low cognitive load (**H**, RM two-way ANOVA, main effect, $F_{1, 16} = 4.914$, $\#p < 0.05$; interaction, $F_{4, 64} = 0.2553$, $p > 0.05$; GFP, $n = 9$; ArchT, $n = 11$), but not under

high cognitive load (**I**, RM 2-way ANOVA, ns $p > 0.05$). **J** Schematic of the experimental design for light stimulation during the "choice" phase. Photoinhibition of DMS D_2R-neurons during the "choice" phase significantly improved WM performance under low cognitive load (**K**, RM two-way ANOVA, main effect, $F_{1, 18} = 4.853$, #$p < 0.05$; interaction, $F_{5, 90} = 0.4557$, $p > 0.05$; Fisher's LSD post-hoc comparisons, Day 3, *$p < 0.05$, Day 4, *$p < 0.05$; $n = 10$ for both groups), but not under high cognitive load (**L**, RM 2-way ANOVA, ns $p > 0.05$). The data underlying panel C can be found in S1 Data. Data are represented as mean ± SEM.

https://doi.org/10.1371/journal.pbio.3003289.g001

induced c-Fos expressions in co-localized cells (Figs 2B, 2C and S1B). During the 10 s "delay" phase, light stimulation of DMS D_2R-neurons with 470 nm laser resulted in impaired WM performance (Fig 2D and 2E). In contrast, under higher cognitive loads (delay 20, 30, and 60 s), optogenetic activation of DMS D_2R-neuron did not significant affect WM (Fig 2F), confirming their selective modulation under condition of low cognitive load. However, activation of D_2R-neurons in a posterior region of the DMS (AP: +0.50 mm) did not lead to significant impairments under both low cognitive load (Fig 2G and 2H) and high cognitive load (Fig 2I). These findings imply that the modulatory effects of D_2R-neurons to WM are topologically specific, consistent with the anterior-posterior gradient of cognitive control in DMS [52]. Locomotion tests indicated no significant differences (S2B Fig). Additionally, chemogenetic activation of DMS D_2R-neurons impaired WM performance, especially under the 10 s delay condition (S3 Fig). In summary, bidirectional optogenetic and chemogenetic experiments corroborate the inhibitory role of DMS D_2R-neurons in WM maintenance and retrieval, particularly under low cognitive load, while their impact on encoding remains negligible.

Optogenetic inhibition of DMS D_1R-neurons selectively improved WM maintenance and retrieval under higher cognitive loads in the T-maze DNMTP task

The effects of optogenetic inhibition of DMS D_1R-neurons on WM maintenance, retrieval, and encoding were investigated across different delay durations. Cre-dependent ArchT-GFP or GFP AAVs were selectively expressed in DMS D_1R-neurons, which projected to GPi and SNR (Fig 3A). Importantly, significant c-Fos induction was observed primarily in ArchT-GFP$^-$ cells due to disinhibition of non-D_1R-neurons (Figs 3B, 3C and S1C).

Under low cognitive load (delay 10 s), optogenetic inhibition of DMS D_1R-neurons during the "sample" (Fig 3D and 3E), "delay" (Fig 3G and 3H), or "choice" (Fig 3J and 3K) phases showed no significant impact on WM performance. In contrast, under higher cognitive loads (delay 20–60 s), optogenetically inhibiting DMS D_1R-neurons during the "delay" (Fig 3I) and "choice" (Fig 3L) phases resulted in notable improvements in WM performance. However, silencing D_1R-neurons during the "sample" phase did not affect WM performance under higher cognitive loads (Fig 3F). Additionally, inhibiting D_1R-neurons resulted in reduced distances traveled in the open field test (S4A Fig). These results show the inhibitory and selective modulation effects of DMS D_1R-neurons on WM maintenance and retrieval, specifically under higher cognitive loads.

Optogenetic activation of DMS D_1R-neurons selectively impaired WM maintenance and retrieval under higher cognitive loads in the T-maze DNMTP task

We further investigated the effects of DMS D_1R-neuron's activation on WM performance. The Cre-dependent targeted expressions of ChR2-mCherry or mCherry in D_1R-neurons were confirmed in Drd1-Cre mice, projecting extensively to SNR (Fig 4A). The c-Fos was significantly increased and mostly co-localized with the virus (Figs 4B, 4C and S1D). Compared to DMS D_2R-neuron's activation (Fig 2E), optogenetic activation of DMS D_1R-neurons during the 10 s "delay" phase did not significantly affect WM performance (Fig 4D and 4E). This finding was further corroborated by chemogenetic activation of DMS D_1R-neurons under low cognitive load condition, which also produced no significant effects (S4 Fig). However, under higher cognitive loads, optogenetic activation of DMS D_1R-neurons during the "delay" phase markedly impaired WM performance (Fig 4F). Without stimulation, there were no significant differences in WM performance (Fig 4G). Open field test revealed insignificant differences upon light activation (pulsed at 5 Hz) of DMS D_1R-neurons (S4B Fig).

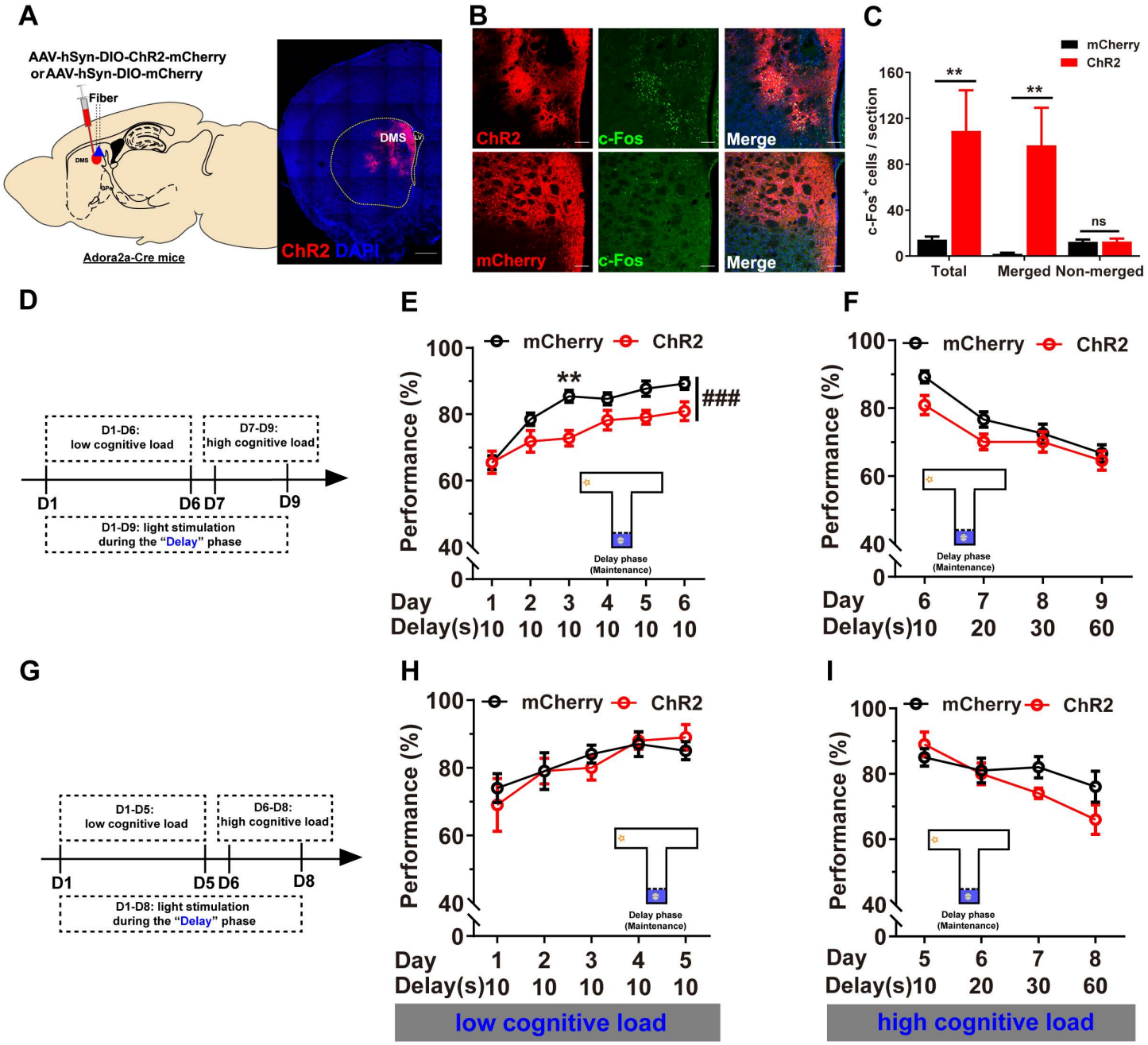

Fig 2. Optogenetic activation of anterior but not posterior D_2R-neurons impaired WM under low cognitive load. A Left: Schematic illustrating virus injection and optic fiber implantation in DMS of Adora2a-Cre (+) mice. Right: Representative images showing ChR2 (red) and DAPI (blue) expression in DMS. **B** Photo-stimulation of ChR2 led to notable c-Fos induction in DMS (green). Scale bar, 100 μm. **C** Quantitative analysis revealed a significant increase in c-Fos expression due to photoactivation of D_2R-neurons, predominantly merged with the virus (Independent Samples *t* test, $^{**}p<0.01$). **D** Schematic of the experimental design for light stimulation during the "delay" phase. **E** During the 10 s "delay" phase, photoactivation of anterior DMS (AP: +0.98 mm) D_2R-neurons significantly impaired WM performance under low cognitive load (RM two-way ANOVA, main effect, $F_{1, 22}=8.79$, $^{\#\#\#}p<0.001$; interaction, $F_{5, 110}=1.635$, $p>0.05$; Bonferroni's post-hoc comparisons, Day 3, $^{**}p<0.01$; mCherry, $n=13$; ChR2, $n=11$). **F** Under high cognitive loads (delay 20, 30, 60 s), photoactivation of anterior DMS (AP: +0.98 mm) D_2R-neurons didn't significantly affect WM performance (RM two-way ANOVA, ns $p>0.05$; mCherry, $n=13$, ChR2, $n=11$). Photoactivation of relatively posterior DMS (AP: +0.50 mm) D_2R-neurons during the "delay" phase didn't affect WM performance under both low (**H**, two-way RM ANOVA, ns $P>0.05$) and high cognitive loads (**I**, two-way RM ANOVA, ns $P>0.05$; $n=10$ for both groups). The data underlying panel C can be found in S1 Data. Data are represented as mean ± SEM.

https://doi.org/10.1371/journal.pbio.3003289.g002

Fig 3. Optogenetic inhibition of D_1R-neurons selectively improved WM maintenance and retrieval under higher cognitive loads. A Top: Schematic illustrating virus injection and optic fiber implantation in DMS of Drd1-Cre (+) mice. Bottom: Representative images showing ArchT expression (green), DAPI staining (blue) in DMS, and its projections to the GPi and SNR. **B** Photoinhibition of ArchT resulted in c-Fos induction in DMS (red). Scale bar, 100 μm. **C** Quantitative analysis demonstrated a significant increase in c-Fos expression due to photoinhibition of D_1R-neurons, primarily in cells

not co-localized with the virus (Independent Samples *t* test, $^{**}p < 0.01$). **D** Schematic of the experimental design for light stimulation during the "sample" phase. Photoinhibition of DMS D_1R-neurons during the "sample" phase did not significantly affect WM under both low (**E**) and high cognitive loads (**F**, RM two-way ANOVA, ns $P > 0.05$; GFP = 10, ArchT = 11). **G** Schematic of the experimental design for light stimulation during the "delay" phase. Photoinhibition of DMS D_1R-neurons during the 10 s "delay" phase did not significantly impact WM performance under low cognitive load (**H**, RM two-way ANOVA, ns $p > 0.05$; GFP = 12, ArchT = 13), but significantly improved WM performance under high cognitive load (**I**, RM two-way ANOVA, main effect, $F_{1, 30} = 14.95$, ###$p < 0.001$; interaction, $F_{3, 69} = 3.690$, $p < 0.05$; Bonferroni's post-hoc comparisons, Delay 60s, ****$p < 0.0001$). **J** Schematic of the experimental design for light stimulation during the "choice" phase. Photoinhibition of DMS D_1R-neurons during the "choice" phase did not significantly impact WM performance under low cognitive load (**K**, RM two-way ANOVA, ns $p > 0.05$; $n = 9$ for both groups), but significantly improved WM performance under high cognitive load (**L**, RM two-way ANOVA, main effect, $F_{1, 16} = 9.066$, ##$p < 0.01$; interaction, $F_{3, 48} = 1.536$, $p > 0.05$; Bonferroni's post-hoc comparisons, Delay 60s, $^{**}p < 0.01$). The data underlying panel C can be found in S1 Data. Data are represented as mean ± SEM.

https://doi.org/10.1371/journal.pbio.3003289.g003

In separate groups of Drd1a-Cre: Ai32 mice, we reduced laser power from ~10 mW to ~1 mW after observing that higher intensities caused unilateral rotation due to asymmetric D_1R-neuron activation (S1 Video). This adjustment eliminated movement bias that could confound WM measurements, particularly during the "choice" phase of our task. Additionally, during this experiment, photo-stimulation was only applied after the mice had learned the task and exhibited stable performance, avoiding potential effects on rule learning during the acquisition stage. The projections of ChR2-EYFP in D_1R-neurons to GPi and SNR were confirmed (Fig 4H), and substantial c-Fos induction was observed (Fig 4I and 4J). As the above optogenetic manipulations were performed during WM task acquisition, to further clarify that DMS D_1R-neurons modulate WM in a cognitive load-dependent manner, rather than learning stage-specific modulation, we refrain from applying light stimulation during the acquisition stage (Fig 4K and 4L). WM performance baselines were comparable between the two groups prior to optogenetic intervention (Fig 4M and 4N, 'before light', black columns). Following this, mild optogenetic activation (1mW) of DMS D_1R-neurons during the "delay" and "choice" phases impaired WM performance, particularly under the 60 s delay (Fig 4N, red and blue columns) but not the 10 s delay (Fig 4M). Optogenetic stimulation during the "sample" phase did not significantly affect WM performance under either cognitive load (Fig 4M and 4N, green columns). Importantly, both groups performed similarly without intervention, indicating that phase-specific manipulations did not influence the animals' rule learning across training days (Fig 4M and 4N, 'light off', gray columns). Additionally, chemogenetic activation of DMS D_1R-neurons didn't influence WM performance under the 10 s delay condition (S5 Fig). These findings highlight the inhibitory and selective modulation effects of DMS D_1R-neurons on WM maintenance and retrieval, particularly under higher cognitive loads. In summary, DMS D_2R-neurons and D_1R-neurons exhibited distinct and dissociable roles in modulating WM: D_2R-neurons selectively regulated WM maintenance and retrieval under low cognitive load, while D_1R-neurons assumed this responsibility under higher cognitive loads. Neither neuronal type influence WM encoding across varying cognitive loads.

Optogenetic inhibition of DMS D_2R-, D_1R-neurons enhanced signal detection sensitivity under low and high cognitive load, respectively, without affecting motivational and motor states in the operant DNMTP task

We further employed an operant-based DNMTP task (Fig 5A) and utilized signal detection theory (SDT) for data analysis [53] (Materials and methods). This approach allowed us to disentangle cognitive processes (sensitivity) from other factors that might influence performance, such as motivational deficits or motor disturbances. According to SDT, task performance is determined by both the sensitivity of neural networks involved in cognitive processes and the motivational or motor output, represented as a bias. Traditional measures, such as percentage correct, do not differentiate between changes in sensitivity and changes in bias. In contrast, SDT provides an effective method for this dissociation [53,54].

The Adora2a-Cre mice expressing either ArchT or GFP in DMS D_2R-neurons were trained on the DNMTP task following a continuous reinforcement (CRF) schedule and the successful acquisition of the non-matching to place (NMTP) rule (Figs 5B and S6A). Subsequent training involved a delayed NMTP procedure with progressively increasing delays (2, 5, 10 s) (Figs 5B and S6B), and no manipulations were introduced during task acquisition to prevent any impacts on rule learning (Fig 5B). Once stable baseline performance was achieved, light stimulation was administered randomly during

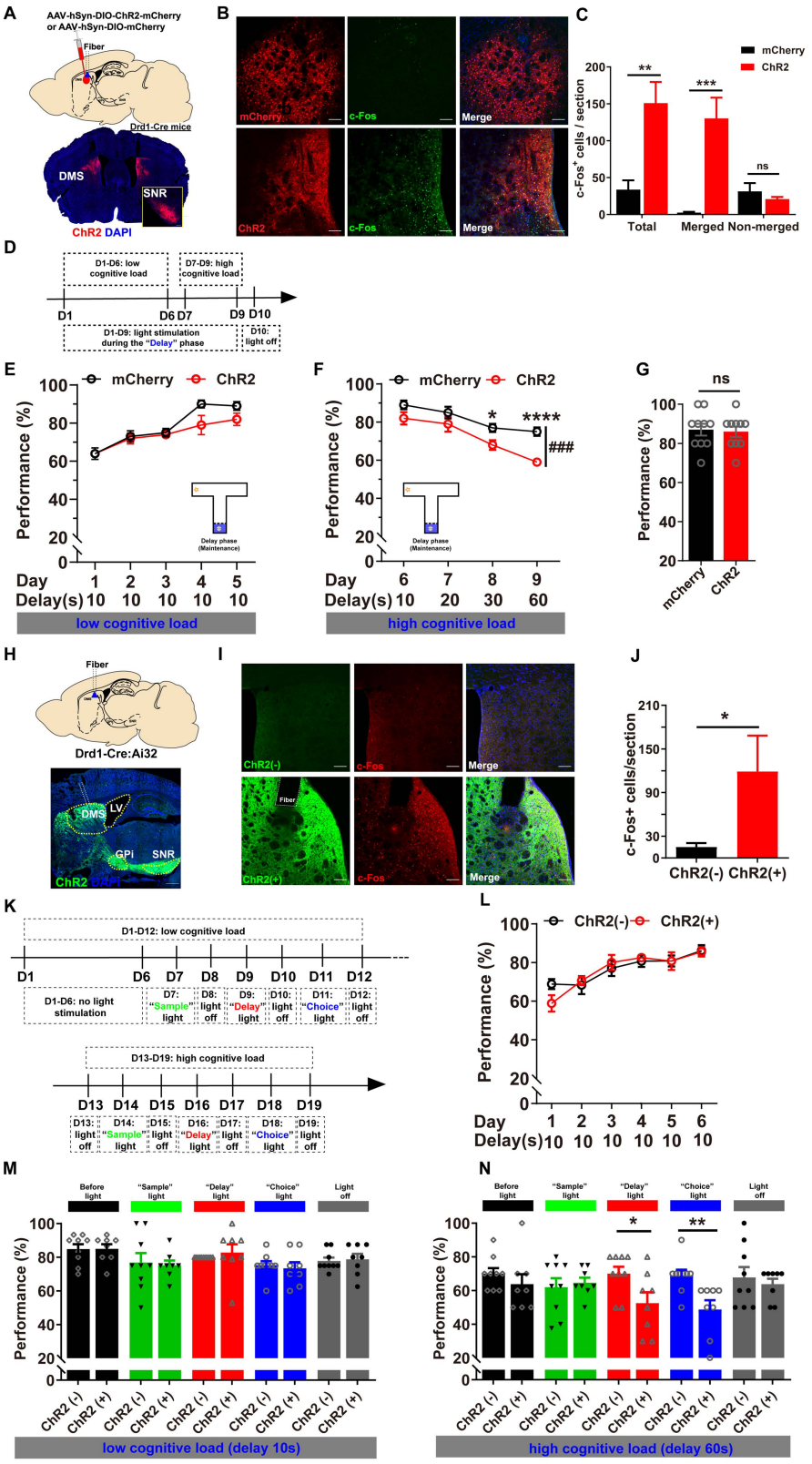

Fig 4. Optogenetic activation of D_1R-neurons selectively impaired WM maintenance and retrieval under higher cognitive loads. A Top: Schematic of virus injection and optic fiber implantation in DMS of Drd1-Cre (+) mice. Bottom: Representative images of ChR2 expression (red) in DMS, with

DAPI staining (blue) and projections in SNR. **B** Photo-stimulation of ChR2 induced c-Fos increase in DMS (green). Scale bar, 100 μm. **C** Quantitative analysis showed significant c-Fos increase due to photoactivation of DMS D_1R-neurons, which was mostly merged with the virus (Independent Samples *T* test, $^{**}p < 0.01$, $^{***}p < 0.001$). **D** Schematic of the experimental design for light stimulation during the "delay" phase. **E** During the 10 s "delay" phase, photoactivation of DMS D_1R-neurons didn't significantly affect WM performance under low cognitive load (RM two-way ANOVA, ns $p > 0.05$; $n = 10$ for both groups). **F** As cognitive loads increased, photoactivation of DMS D_1R-neurons during the "delay" phase significantly impaired WM performance (RM two-way ANOVA, ### $p < 0.001$; Bonferroni's post-hoc comparisons, delay 30 s, $^{*}p < 0.05$, delay 60 s, $^{****}p < 0.0001$). **G** Without stimulation, there were no significant differences in WM performance (Independent Samples *T* test, ns $p > 0.05$). **H** Top: Schematic of optic fiber implantation in DMS of Drd1a-Cre/Ai32 mice. Bottom: Representative images of ChR2 expression (green) in DMS, with DAPI staining (blue) and projections into GPi and SNR. **I** Photo-stimulation of ChR2 induced c-Fos expression in DMS (red). Scale bar, 100 μm. **J** Quantitative analysis revealed a significant increase in c-Fos expression due to photoactivation of DMS D_1R-neurons (Independent Samples *T* test, $^{*}p < 0.05$). **K** Schematic of the experimental design for light stimulation during the "sample", "delay" or "choice" phase. **L** No light was delivered during the task acquisition stage (Day 1-6). **M** Under the 10 s delay condition (low cognitive load), mild photoactivation (~1 mW) of DMS D_1R-neurons during the "sample", "delay" or "choice" phases did not significantly impact WM performance. **N** Under the 60 s delay condition (high cognitive load), mild photoactivation during the "delay" and "choice" phases markedly impaired WM performance, whereas activation during the "sample" phase had no effect (Independent Samples *t* test, "Delay light": $^{*}p < 0.05$, "Choice light": $^{**}p < 0.01$; ChR2 (−) = 9, ChR2 (+) = 8). The data underlying panels C, G, J, M, and N can be found in S1 Data. Data are represented as mean ± SEM.

https://doi.org/10.1371/journal.pbio.3003289.g004

the "sample", "delay" or "choice" phase (Fig 5B). Optogenetically inhibiting DMS D_2R-neurons during the "sample" phase did not impact sensitivity (correct percentage, Fig 5C; SI and 5D), bias measures (RI, Fig 5E), or responsivity measures (latency to the sample lever, LS, S6C Fig; latency to the choice lever, LC, S6D Fig), although it did increase nose pokes during the "delay" phase (S6E Fig). Specifically, optogenetic inhibition of DMS D_2R-neurons significantly improved the percentage of correct responses, particularly at shorter delays (2 and 5 s, Fig 5F). The sensitivity index (SI) derived from SDT analysis also showed significant enhancement, especially under the 2 s delay condition (Fig 5G). A higher SI indicates improved discrimination between signal and noise, suggesting enhanced WM performance [53,54]. Furthermore, optogenetic inhibition of DMS D_2R-neurons during the "delay" phase did not lead to motor disturbance, as indicated by bias measures (responsivity index, RI, Fig 5H), nor did it affect motivational state, as reflected by responsivity measures (LS, S6F Fig; LC, S6G Fig; and nose pokes during the delay phase, S6H Fig).

During the "choice" phase, optogenetic inhibition of DMS D_2R-neurons again improved both the percentage of correct responses (Fig 5I) and the SI (Fig 5J). However, there were no significant differences observed in bias measures (RI, Fig 5K) or responsivity measures (LS, S6I Fig; nose pokes, S6K Fig) between the groups. However, light stimulation during the "choice" phase increased LC, particularly under the 10 s delay condition (S6J Fig), indicating potential laser interference with the animals' decision-making process. However, there were no significant changes in the correct percentage or SI under the 10 s condition (Fig 5I and 5J), suggesting that the WM component remained unaffected despite longer choice latency. Collectively, optogenetic inhibition of DMS D_2R-neurons during the "delay" and "choice" phases significantly enhanced WM signal detection sensitivity, particularly under low cognitive load, without impacting motivational and motor states.

Moreover, Drd1-Cre: Ai35 mice, including ArchT-expressing ($ArchT^+$) and non-expressing ($ArchT^-$) groups, underwent training in the operant DNMTP task without light manipulations during the CRF, NMTP (S6L Fig), and DNMTP training (S6M Fig). Following this, light stimulation was administered randomly during the "sample", "delay", or "choice" phase (Fig 5B). Optogenetic inhibition of DMS D_1R-neurons during the "sample" phase did not significantly influence any of the measured outcomes (Figs 5L–5N and S6N–S6P). However, optogenetic inhibition of DMS D_1R-neurons during the "delay" and "choice" phases led to significant improvements under the 10 s delay condition in both the percentage of correct responses (Fig 5O for "Delay light," Fig 5R for "Choice light") and signal sensitivity (SI, Fig 5P for "Delay light," Fig 5S for "Choice light"). Importantly, there were no significant differences in bias measure (RI, Fig 5Q "Delay light," Fig 5T for "Choice light") or responsivity measures (LS, S6Q Fig for "Delay light," S6T Fig for "Choice light"; LC, S6R Fig for "Delay light," S6U Fig for "Choice light"; Nose pokes, S6S Fig for "Delay light," S6V Fig for "Choice light") between the groups, indicating that motivational and motor states remained unaffected. So, optogenetically inhibiting DMS D_1R-neurons during the "delay" and "choice" phases resulted in improved WM signal detection sensitivity, particularly under higher cognitive

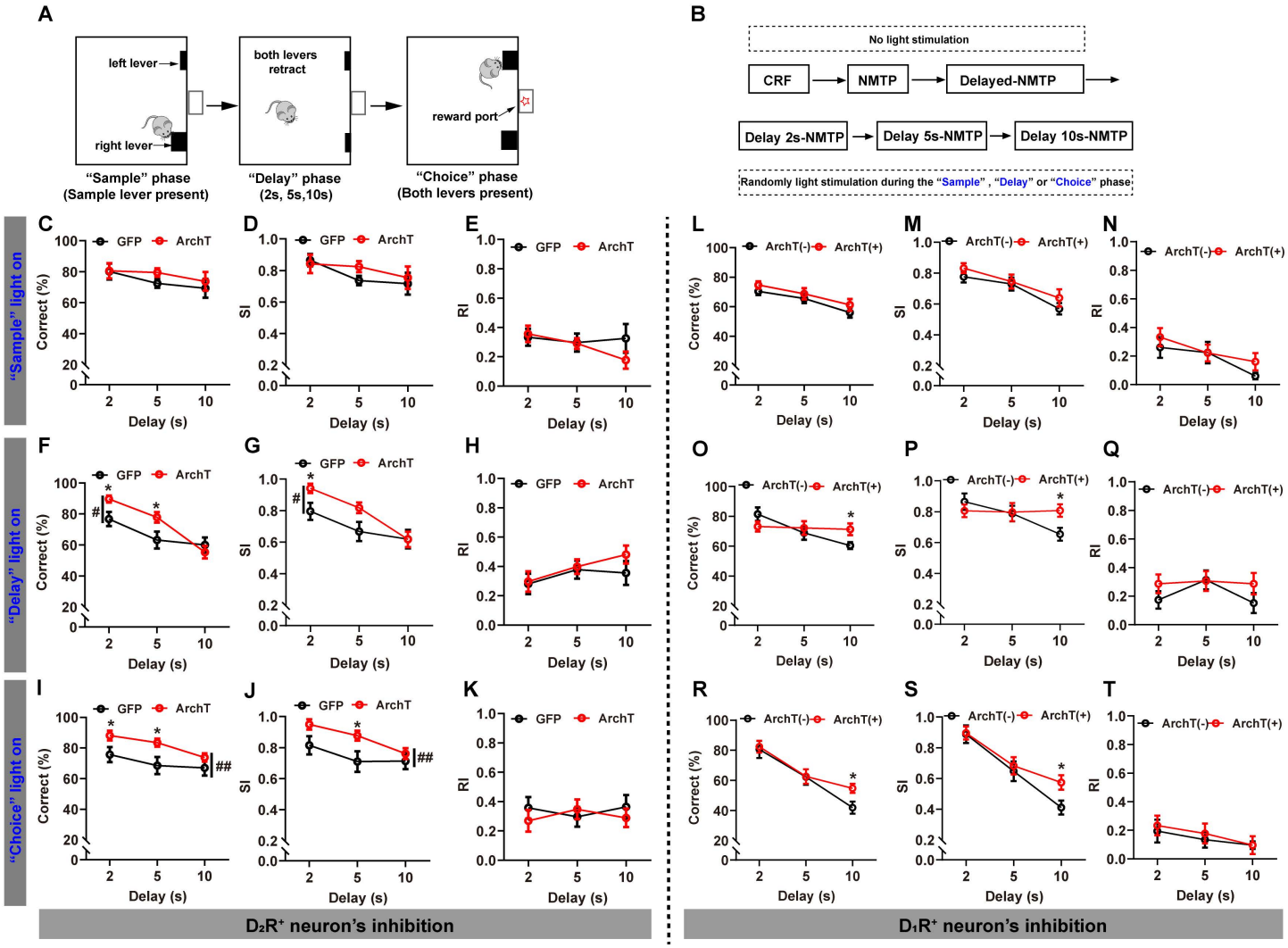

Fig 5. Optogenetic inhibition of D_2R-, D_1R-neurons enhanced signal detection sensitivity under low and high cognitive load, respectively, without affecting motivational and motor states in the operant DNMTP task. A Schematic representation of the operant DNMTP task. **B** Schematic of the experimental design for light stimulation during the operant DNMTP task. **C–E** During the "sample" phase, photoinhibition of DMS D_2R-neurons didn't significantly impact the percentages of correct responses (**C**), SI (**D**) and RI (**E,** RM two-way ANOVA, $p > 0.05$). **F–H** During the "delay" phase, photoinhibition of DMS D_2R-neurons significantly improved the percentage of correct responses (**F**) and SI (**G**), particularly at 2 and 5 s delays (**F**: RM two-way ANOVA, main effect, $F_{1, 54} = 4.255$, #$p < 0.05$; interaction, $F_{2, 54} = 3.024$, $p = 0.0569$; Fisher's LSD post-hoc comparisons, Delay 2 s, *$p < 0.05$, Delay 5 s, *$p < 0.05$; **G**: RM two-way ANOVA, main effect, $F_{1, 54} = 5.091$, #$p < 0.05$; interaction, $F_{2, 54} = 1.434$, $p > 0.05$; Fisher's LSD post-hoc comparisons, Delay 2 s, *$p < 0.05$), but didn't significantly affect RI (**H**). **I–K** During the "choice" phase, photoinhibition of DMS D_2R-neurons significantly enhanced the percentage of correct responses (**I**, RM two-way ANOVA, main effect, $F_{1, 54} = 10.72$, ##$p < 0.01$; interaction, $F_{2, 54} = 0.4727$, $p > 0.05$; Fisher's LSD post-hoc comparisons, Delay 2 s, *$p = 0.0504$, Delay 5 s, *$p < 0.05$) and SI (**J**, RM two-way ANOVA, main effect, $F_{1, 54} = 8.527$, ##$p < 0.01$; interaction, $F_{2, 54} = 0.7768$, $p > 0.05$; Fisher's LSD post-hoc comparisons, Delay 5 s, *$p < 0.05$), particularly notable at 2 and 5 s delays. However, there were no significant changes in RI (K). Sample sizes: GFP, $n = 8$, ArchT, $n = 9$. **L–N** During the "sample" phase, photoinhibition of DMS D_1R-neurons had no significant effects on the percentage of correct responses (**L**), SI (**M**), and RI (*N*). **O–Q** During the "delay" phase, photoinhibition of DMS D_1R-neurons significantly improved the percentage of correct responses (**O**, Independent *T* test, delay 10 s, *$p < 0.05$) and SI (**P**, Independent *T* test, Delay 10 s, *$p < 0.05$) of WM during the 10 s delay. However, photoinhibition didn't affect RI (**Q**). **R–T** During the "choice" phase, photoinhibition of DMS D_1R-neurons significantly improved the percentage of correct responses (**R**, Independent *T* test, delay 10 s, *$p < 0.05$) and SI (**S**, Independent *T* test, Delay 10 s, *$p < 0.05$) under the 10 s delay condition. Photoinhibition of DMS D_1R-neurons during the "choice" phase didn't impact RI (**T**). Sample sizes: ArchT(+), $n = 9$, ArchT(−), $n = 9$. Data are presented as mean ± SEM.

https://doi.org/10.1371/journal.pbio.3003289.g005

loads. In summary, optogenetic inhibition of DMS D_2R-, D_1R-neurons enhanced signal detection sensitivity under low and high cognitive load, respectively, without affecting motivational and motor states in the operant DNMTP task, which further corroborated DMS D_1R- and D_2R- neuron's cognitive load-dependent modulation on WM.

It's worth noting that although early interventions during the training stage in the T-maze could potentially influence rule acquisition, the replication of our key findings in the operant DNMTP task—where manipulations were introduced only after stable task acquisition—supports the conclusion that the observed effects are predominantly due to modulation of WM maintenance and retrieval, rather than alterations in the learning processes.

Optogenetic and pharmacological inhibition of dopamine signaling rescued WM impairment induced by the activation of DMS D_1R-neurons

We demonstrated that optogenetic silencing of DMS D_1R-neurons enhanced WM performance, whereas their activation impaired WM. This inhibitory modulation of DMS D_1R-neurons on WM contrasts with previous studies emphasizing their facilitating role in goal-directed behavior, action selection, and associative learning [26–30,55,56]. Higher dopamine tone in the mPFC promotes stability of WM representations [57], whereas striatal dopamine acts as a gatekeeper—elevated striatal dopamine facilitates the updating of new information, but disrupts the stabilization of existing content [58,59]. We hypothesized that under higher cognitive load, excessive dopamine in the DMS during the "delay" phase may activate D_1R-neurons and thereby impair WM. To test this, we performed rescue experiments investigating whether WM deficits caused by DMS D1R-neuron activation could be alleviated through: (1) optogenetically blocking midbrain dopaminergic neuron activity; (2) inhibiting dopaminergic terminal release in the DMS, 3) pharmacologically blocking dopamine D1 receptors.

First, we examined whether optogenetic inhibition of dopaminergic neurons in the VTA and SNc during the "delay" period could alleviate WM impairment caused by DMS D_1R-neuron activation under higher cognitive loads (Fig 6A). To this end, Cre-dependent AAVs were introduced to express ChR2-EYFP in DMS D_1R-neurons (Fig 6B, left) of Drd1-Cre mice. We specifically targeted dopaminergic neurons in the VTA/SNc using ArchT-mCherry AAVs driven by the mouse tyrosine hydroxylase (mTH) promoter (Fig 6B, right). Immunohistochemical staining of TH confirmed the selective expressions of ArchT-mCherry in VTA/SNc dopaminergic neurons (Fig 6B, right). Quantitative analysis demonstrated that 73.25–84.51% of the virus colocalized with TH^+ neurons in the VTA/SNc across bregma −3.16 to −3.64 mm (S7 Fig), which are comparable to those reported in the literatures using similar mTH promoter-driven strategies [60,61]. However, this specificity is lower than the ~96% typically achieved using DAT-Cre mice [62], which represents the most selective approach for targeting dopaminergic neurons. We found that optogenetic activation of D_1R-neurons during the 60 s "delay" period significantly impaired WM performance (Fig 6C). However, optogenetic inhibition of dopamine neurons in VTA/SNc successfully rescued this impairment (Fig 6D). Notably, the group undergoing dual stimulation (DMS ChR2 + VTA/SNc ArchT) demonstrated significant WM improvement compared to those receiving single stimulation (activation of DMS D_1R-neurons) (Fig 6E). This group also showed enhanced performance relative to the DMS (ChR2 + VTA/SNc mCherry) group and exhibited no significant differences compared to the control group (DMS EYFP + VTA/SNc mCherry, Fig 6E). These results indicated that suppressing DMS dopamine signaling during the "delay" phase effectively rescues WM impairment induced by the activation of DMS D_1R-neurons under higher cognitive loads. Importantly, rule learning remained unaffected by these manipulations as the WM performance of the three groups shows no significant difference when withdrawing light stimulation (Fig 6F).

Next, we investigated whether optogenetic inhibition of VTA/SNc dopamine projection terminals in DMS during the "delay" phase could reverse WM impairment induced by the activation of D_1R-neuron. Using a similar viral expression strategy as in the first experiment, we implanted a twin-core optic fiber in DMS for dual stimulation (Fig 6G). Targeted expressions of ArchT-mCherry in dopaminergic neurons and ChR2-EYFP in DMS D_1R-neurons were confirmed (Fig 6H). Recent work suggests that under certain conditions, optogenetic inhibition with ArchT at presynaptic terminals may

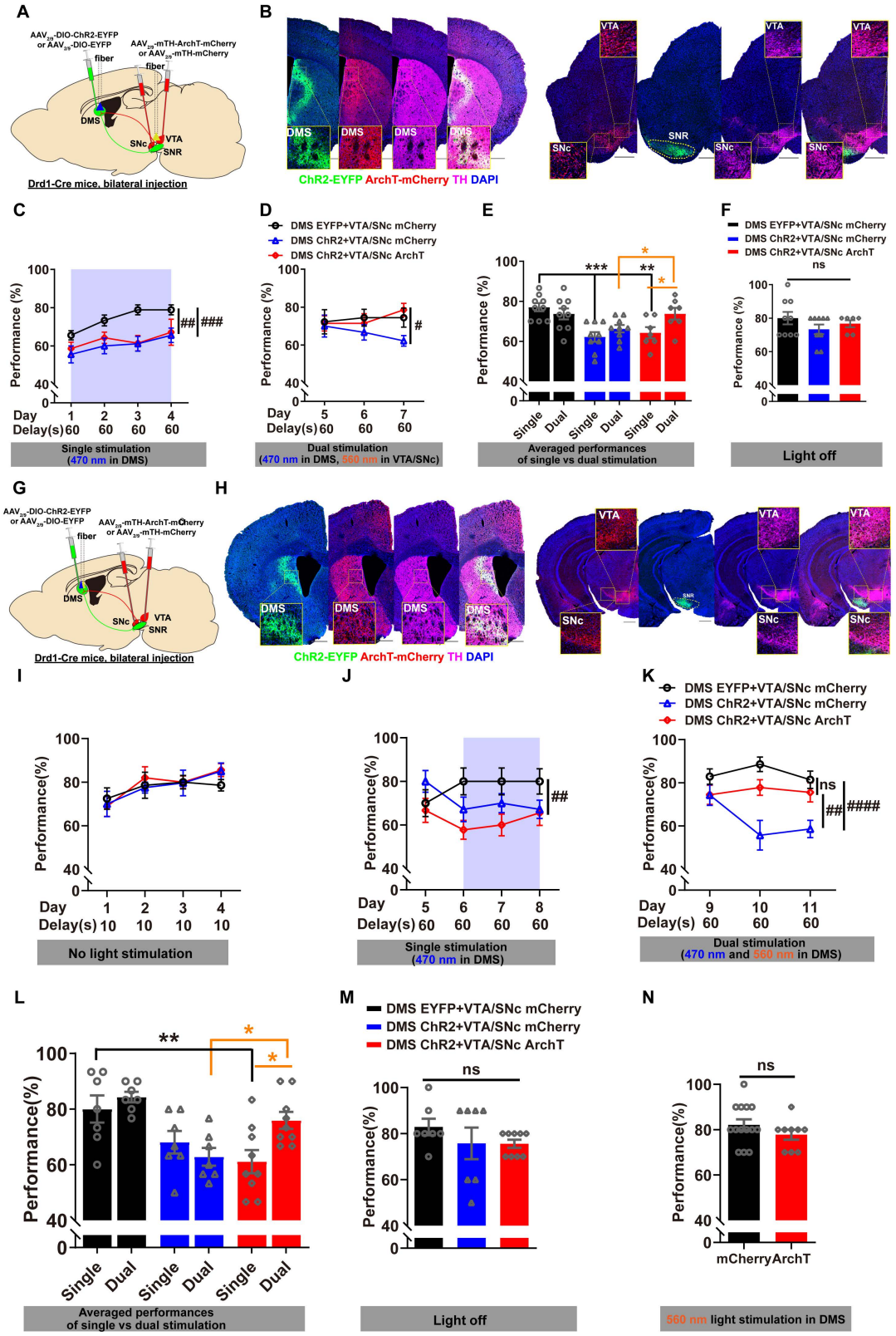

Fig 6. Optogenetic inhibition of DMS dopamine signaling rescue WM impairment induced by D_1R-neuron activation. A Schematic illustrating the viral injection of DIO-ChR2-EYFP or DIO-EYFP, along with the implantation of optic fiber in DMS, and the injection of mTH-ArchT-mCherry

or mTH-mCherry, with optic fiber implantation in VTA/SNc of Drd1-Cre (+) mice. **B** Left: Representative images displaying ChR2 expression (green), ArchT fibers from VTA/SNc (red), alongside TH staining (magenta) and DAPI (blue) in DMS; Right: Representative images in VTA/SNc showing ArchT expression (red), ChR2 projections in SNR (green), TH staining (magenta) and DAPI (blue) in VTA/SNc. ArchT was selectively expressed in TH-positive dopaminergic neurons. **C** During the 60 s "delay" phase, photoactivation of DMS D_1R-neurons with 470 nm laser severely impaired WM performance (Group 1 'DMS EYFP + VTA/SNc mCherry' vs. Group 3 'DMS ChR2 + VTA/SNc ArchT': RM two-way ANOVA, main effect, $F_{1, 14} = 15.92$, ##$p < 0.01$; interaction, $F_{3, 24} = 0.9179$, $p > 0.05$; Fisher's LSD post-hoc comparisons, Day 2, *$p < 0.05$, Day 3, **$p < 0.01$; Group 1 'DMS EYFP + VTA/SNc mCherry' vs. Group 2 'DMS ChR2 + VTA/SNc mCherry': RM two-way ANOVA, main effect, $F_{1, 16} = 20.22$, ###$p < 0.001$; interaction, $F_{3, 48} = 0.5375$, $p > 0.05$; Fisher's LSD post-hoc comparisons, Day 2, *$p < 0.05$, Day 3, **$p < 0.01$, Day 4, *$p < 0.05$). **D** During the "delay" phase, photoinhibition of dopaminergic neurons in VTA/SNc (red prismatic) with 560 nm laser effectively rescued D_1R-neuron activation-induced WM impairment, yielding performance comparable to the control group (black circle) (Group 2 'DMS ChR2 + VTA/SNc mCherry' vs. Group 3 'DMS ChR2 + VTA/SNc ArchT': RM two-way ANOVA, main effect, $F_{1, 14} = 5.024$, #$p < 0.05$; interaction, $F_{2, 48} = 1.485$, $p > 0.05$; Fisher's LSD post-hoc comparisons, Day 7, **$p < 0.01$). **E** In Group 3, dual stimulation significantly improved WM performance compared to single stimulation (red column). Additionally, it demonstrated notable enhancements over Group 2, with no significant difference with Group 1 (One-way ANOVA for comparisons among the three groups; Paired-samples *t* test for group 3's comparisons between single and dual stimulation; Group 1, $n = 9$, Group 2, $n = 9$, Group 3, $n = 7$). **F** Without interventions, WM performance among the three groups was comparable, showing no significant differences. **G** The viral injection strategy was similar to that described in panel A. Twin-core optic fibers were implanted into DMS to activate D_1R-neurons and inhibit DMS dopaminergic terminals, either respectively or simultaneously. **H** Left: Representative images showing ChR2 expression (green), ArchT fibers from VTA/SNc (red), TH staining (magenta), and DAPI (blue) in DMS; Right: Representative images VTA/SNc showing ArchT expression (red), ChR2 fibers in SNR from DMS (green), TH staining (magenta), and DAPI (blue). ArchT was selectively expressed in TH-positive dopaminergic neurons VTA/SNc. **I** WM performances of the three groups were comparable without manipulations during the learning stage (Day 1–4). **J** During the 60 s "delay" phase, photoactivation of DMS D_1R-neurons with 470 nm laser severely impaired WM performance (Group 1 'DMS EYFP + VTA/SNc mCherry' vs. Group 3 'DMS ChR2 + VTA/SNc ArchT': RM two-way ANOVA, main effect, $F_{1, 56} = 14.20$, ## $p < 0.01$; interaction, $F_{3, 56} = 1.123$, $p > 0.05$; Fisher's LSD post-hoc comparisons, Day 6, **$p < 0.01$, Day 7, *$p < 0.05$). **K** During the "delay" phase, photoinhibition of DMS dopaminergic terminals with 560 nm laser (red prismatic) successfully rescued WM impairment induced by D_1R-neuron activation, yielding performance comparable to the control group (black circle) (Group 3 vs. Group 1: RM two-way ANOVA, main effect, $F_{1, 14} = 4.751$, $p > 0.05$, interaction, $F_{2, 28} = 0.2166$, $p > 0.05$; Group 3 vs. Group 2 'DMS ChR2 + VTA/SNc mCherry': RM two-way ANOVA, main effect, $F_{1, 42} = 11.41$, ## $p < 0.01$, interaction, $F_{2, 42} = 2.926$, $p > 0.05$, Fisher's LSD post-hoc comparisons, Day 10, **$p < 0.01$, Day 11, *$p < 0.05$; Group 1 vs. Group 2: RM two-way ANOVA, main effect, $F_{1, 36} = 32.49$, #### $p < 0.0001$, interaction, $F_{2, 36} = 3.513$, $p < 0.05$, Bonferroni's post-hoc comparisons, Day 10, **** $p < 0.0001$, Day 11, ** $p < 0.01$). **L** In Group 3, dual stimulation resulted in a significant enhancement of WM performance compared to single stimulation (red column). Group 3 demonstrated notable improvement over Group 2, with no significant differences compared to Group 1 (One-way ANOVA for the comparisons of the three groups; Paired-samples *t* test for Group 3's comparisons between single stimulation and dual stimulation; Group 1, $n = 7$, Group 2, $n = 7$, Group 3, $n = 9$). **M** Without manipulations, no significant differences in performance were observed among the three groups (One-way ANOVA, ns, $p > 0.05$). **N** Photoinhibition of dopaminergic terminals in DMS alone had no significant impact on WM performance (Independent Samples *t* test, $p > 0.05$). The data underlying panels E, F, L, M, and N can be found in S1 Data. Data are presented as mean ± SEM.

https://doi.org/10.1371/journal.pbio.3003289.g006

enhance, rather than reduce neurotransmitter release [63]. We performed two experiments to determine the effects of ArchT stimulation of dopaminergic terminal in the DMS on the neuronal activity and synaptic dopamine release. First, AAV-mTH-ArchT-mCherry and AAV-mTH-GCaMP6m were injected into the SNc and VTA, with two optical fibers obliquely implanted in the DMS—one for 560 nm light stimulation of ArchT and the other for recording calcium signal. Second, AAV-mTH-ArchT-mCherry was injected into the SNc and VTA, and a dopamine sensor virus (AAV-hSyn-DA1h) into the DMS, with similar fiber placement to record dopamine release. Optogenetic activation of ArchT in these terminals for 60 seconds resulted in significant reductions in both calcium and dopamine signals in the DMS (S8C and S8F Fig).

Following successful learning without intervention (Fig 6I), activating DMS D_1R-neurons during the 60 s "delay" period reproduced WM impairment (Fig 6J). However, optogenetic inhibition of dopaminergic terminals in DMS led to significant WM performance improvements, comparable to the control group (Fig 6K). In Group 3 (DMS ChR2 + VTA/SNc ArchT), dual stimulation (470 nm + 560 nm) demonstrated significantly enhancement over single stimulation (473 nm) (Fig 6L). It displayed notable improvement compared to Group 2 (DMS ChR2 + VTA/SNc mCherry (Fig 6K and 6L). No significant differences between the groups were observed without interventions (Fig 6M). Additionally, inhibiting DMS dopaminergic terminals alone did not yield significant differences, indicating that dopamine inhibition can only rescue functional deficiencies under conditions of WM impairments, such as in pathological states (Fig 6N).

Finally, we assessed whether pharmacological inhibition of D_1R or D_2R which are highly expressed in the striatum, could counteract WM impairment resulting from DMS D_1R-neuron's activation. Optogenetic activation of DMS D_1R-neurons during the 60 s "delay" phase significantly impaired WM performance (S9B Fig). Notably, intraperitoneal injection

of the D_1R antagonist SCH39166 partially rescued this impairment (S9C Fig), whereas the D_2R antagonist Sulpiride had no effect (S9D Fig). Without interventions, both groups performed similarly (S9E Fig).

In summary, optogenetic inhibition of the midbrain dopamine neurons, or the dopaminergic projection terminals in DMS, or pharmacological antagonism of D_1R (but not D_2R) effectively ameliorated WM impairment induced by DMS D_1R-neuron activation during the "delay" phase. These findings confirm the inhibitory effects of DMS dopamine signaling on WM under conditions of heightened cognitive load.

Discussion

Through bidirectional optogenetic manipulations of D_1R- and D_2R-neurons during specific phases under varying cognitive loads, we have demonstrated the distinguishing characteristics that DMS D_1R- and D_2R-neurons regulate WM: (1) phase-specific control: both neuronal types selectively modulate the maintenance and retrieval of WM, with no significant impact on the encoding process. Utilizing SDT analysis, we further confirmed that these two neuronal populations specifically modulate WM signal detection sensitivity, independent of motivational or motor influences; (2) "relay" control: remarkably, DMS D_1R- and D_2R-neurons functioned in a coordinated manner, demonstrating a cognitive load-dependent "relay" mechanism. Under conditions of low cognitive load, WM is predominantly regulated by DMS D_2R-neurons, while the responsibility shifts to DMS D_1R-neurons as the cognitive load increases; (3) inhibitory control: Activation of DMS D_1R-neurons during the delay phase severely impairs WM under high cognitive load, which is alleviated by optogenetic inhibition of the midbrain dopaminergic neurons, or dopaminergic terminals in DMS, or administration of a D_1R antagonist (but not a D_2R antagonist). Collectively, our findings unveil a "relay" model of inhibitory control by DMS neurons over WM maintenance and retrieval, highlighting a cognitive load-dependent transition from D_2R- to D_1R-neurons. This model elucidates the dynamic cellular mechanism that underpin the collaborative and complementary roles of these two DMS neuronal populations, ensuring continuous regulation of WM.

Cognitive load-dependent switch from DMS D_2R- to D_1R-neurons confers continuous and complementary modulation of WM

The understanding of BG function has evolved, shifting from the traditional "go/no-go" model [31,32] to "complementary" [24,25] and "competitive" frameworks [33], elucidating the BG's intricate roles in procedural learning [34]. Yet, the interplay between D_1R and D_2R-neurons in declarative learning, particularly within the realm of WM [35], remains unexplored. In this study, we propose a novel "relay" model that indicates a cognitive-load dependent transition from D_2R- to D_1R-neurons, facilitating continuous and coordinated control of WM maintenance and retrieval. Specifically, during the 10 s delay in the DNMTP task, the optogenetic silencing of D_2R-neurons resulted in improved WM performance, while their activation diminished performance. Interestingly, manipulating D_1R-neurons showed no significant effect. However, in tasks requiring longer memory durations (20–60 s), D_1R-neurons took over the role of effective control. This represents the first evidence of a "relay" control mechanism in WM, wherein D_2R-neurons are supplanted by D_1R-neurons to provide continuity in response to elevated cognitive loads.

Our investigation of DMS control of WM aligns with and extends the important findings from Bolkan and colleagues regarding pathway-specific behavioral regulation [64]. Both emphasize the context-dependent engagement of striatal pathways. Bolkan and colleagues focus on behavioral strategies and evidence accumulation, demonstrating that striatal pathway contributions vary with internal state even within the same task. Our work specifically addresses the dynamic roles of DMS pathways in different WM processes under varying cognitive loads. Together, these results demonstrate that striatal contributions are flexibly and dynamically tuned by both external demands and internal conditions, moving beyond classic "go/no-go" models toward a more nuanced, adaptive view of striatal circuit function.

Given that WM has limited capacity and rapidly deteriorate within seconds, longer delay intervals correspond with decreased WM recall performance [45,65]. According to the time-based resource-sharing model of WM [43], cognitive

load is a function of the time needed for specific activities to capture attention [66]. As delays increase, the spiking activities declines according to the time-related memory traces decay model [66], or the sustained active regions, like bump attractors, drift over time due to noise, as described in the drift model [67,68]. Heightened cognitive load stimulates these putative neuronal substrates of WM, driving the shift from DMS D_2R- to D_1R-neurons for dynamic network control. This is corroborated by studies showcasing transient neural firing among different populations during consistent WM delay duration [69] and the sequential activation of D_1R and D_2R neuronal ensembles during motor learning [26]. The selective regulation of DMS D_1R-neurons under heightened cognitive loads lays a foundation for strategies aimed at enhancing WM capacity through the modulation of these specific neuronal populations.

Complementary and inhibitory modulation of WM by DMS D_1R- and D_2R-neurons

Our investigation demonstrates that DMS D_1R- and D_2R-neurons work in a coordinated and inhibitory manner to modulate WM. Experimental manipulations revealed that optogenetic silencing of either DMS D_1R- or D_2R-neurons during the "delay" and "choice" phases resulted in enhanced WM performance, while their activation disrupted WM. Although DMS D_1R-neurons are generally associated with facilitating motor and reward-based behaviors, their activation may heighten sensory inputs into DMS, which could interfere with WM maintenance and retrieval processes. This inhibitory mechanism aligns with previous studies indicating that overexpression of D_2Rs in the striatum increases striatal excitability yet impairs WM efficacy [70–73]. By maintaining DMS in a suppressive state, the WM gate threshold is elevated, which restricts new information updating while promoting the maintenance and retrieval of existing information in the cortex. These findings hold clinical implications, suggesting that selectively inhibiting DMS activity through non-invasive methods may enhance WM in older individuals and those with neuropsychiatric disorders characterized by WM impairments.

Materials and methods

Animals

All animal care and experimental procedures adhered to the National Institutes of Health Guide for the Care and Use of Laboratory Animals. Ethical approval was obtained from the Institutional Ethics Committee for Animal Use in Research and Education at Wenzhou Medical University, China (approval/license number: xmsq2023-0236). Drd1a-Cre mice (No. 034258-UCD) and Adora2a-Cre mice (No. 031168-UCD) were procured from the Mutant Mouse Resource & Research Centers, while Ai32 (No. 012569) and Ai35 (No. 012735) mice were sourced from the Jackson Laboratory. Transgenic lines, Drd1a-Cre:Ai32 and Drd1a-Cre:Ai35, were generated by crossing Drd1a-Cre with Ai32 or Ai35 mice, respectively. The mice, aged 8–12 weeks, were housed under a 12-hour light/dark cycle with *ad libitum* access to food and water.

Optogenetic manipulations coupled with T-maze DNMTP task

The T-maze DNMTP task, widely utilized to assess spatial WM [37–41,74], was performed with minor modifications [48,75]. After a 2-week recovery period, mice underwent a food restriction regimen to maintain their body weight at approximately 85% of their original weight. Over three days, a 10-min free exploration and foraging period was conducted to familiarize the mice with the maze. Following this acclimatization, mice performed 10 trials per session on the DNMTP task, with each trial consisting of three phases: sample, delay, and choice.

During the sample phase, one randomly selected arm of the maze was blocked, allowing the mouse to explore the open arm and receive a sucrose solution reward. The location of the sample arm was encoded during this phase (encoding). In the delay phase, the mouse was required to retain the sample arm location online for a variable duration (maintenance). The choice phase involved the mouse selecting the previously unexplored arm to receive a second reward (retrieval), indicative of a correct trial.

The DNMTP task permitted flexible adjustments to the difficulty level [48], with increasing delay intervals necessitating that the animal retain location information for longer, thereby intensifying cognitive load. WM performance was observed to decline as the delay period lengthened, which is a hallmark characteristic of WM [76]. Mice underwent initial training with a 10 s delay and were required to achieve over 85% success within 5–6 days. Upon successful acquisition, the delay was progressively extended to 20, 30, and 60 s, resulting in decreased performance with longer delays.

To investigate the roles of DMS D_1R- or D_2R-neurons in the encoding, maintenance, and/or retrieval phases of spatial WM, optogenetic manipulations were employed during each phase (sample, delay, choice). Neurons were activated using 473 nm blue light pulsed at 5 Hz with 80 ms pulse width (10 mW or 1 mW laser power), while inhibition was achieved with continuous 563 nm light (10 mW laser power). The duration of light stimulation during the "sample" or "choice" phase varied slightly across trials, generally ranging from 10 to 15 s. During the delay period, the light stimulation duration corresponded to the specific "delay" duration.

Optogenetic manipulations coupled with operant DNMTP task

The automated murine operant DNMTP task was utilized to investigate the effects of optogenetic manipulations on DMS D_1R- or D_2R-neurons in spatial WM, based on previously established protocols with minor adjustments [77,78]. Following a two-week recovery period, mice underwent food restriction and were acclimatized to the operant chambers (Med Associates) during three 15-min sessions. Each nose poke into the food port resulted in a reward of 20 μL of a 20% sucrose solution. This was followed by a series of 5–7 CRF sessions, consisting of 50 trials per session, in which left and right levers were randomly presented for a maximum duration of 30 min; each lever press yielded a reward of 20 μL of the 20% sucrose solution. Once the animals consistently consumed the rewards, training on the NMTP task began, with each session consisting of 50 trials. In the sample phase, either the left or right lever was presented in a pseudorandom order. After the mouse pressed the lever, it retracted, and the first nose poke into the food port triggered the presentation of both levers (choice phase). Choosing the lever that had not presented in the sample phase was considered a correct response, resulting in reward delivery and lever retraction. If no response was made within 15 s, both levers retracted, and the trial was labeled as an "Omission". During initial training, 30 correction trials were conducted to address positional bias in the choice phase. Once the mice achieved a correct response rate exceeding 80% for three consecutive sessions, delays of 2, 5, 10, and 20 seconds were introduced between the sample and choice phases, with 16 trials per delay, presented in a randomized order. In the DNMTP stage, the first nose poke after the delay period presented the choice levers. Incorrect lever presses or failure to respond within 15 s resulted in a 5-s time-out penalty, followed by a 10-second inter-trial interval.

After seven sessions of DNMTP training, stable baseline responses were attained. Subsequently, optogenetic manipulations of DMS D_1R- or D_2R-neurons were performed using different set of mice. Light was delivered randomly during the "sample", "delay" or "choice" phase of each trial. The duration of light stimulation during the "sample" or "choice" phase varied slightly across trials, typically ranging from 5 to 10 s. During the delay period, the length of light stimulation corresponds to the duration of the delay. Notably, at the 20-s delay interval of the operant DNMTP task, mice may employ various strategies (such as cue-based or egocentric strategies) alongside the spatial strategy mediated by WM [79]. Performance at the 2, 5, and 10-second delays was subsequently analyzed.

Operant DNMTP behavioral data analysis using SDT

Behavioral measures from the operant DNMTP task were recorded and analyzed according to established protocols [53]. Key metrics evaluated during the shaping phase and throughout the NMTP and DNMTP stages included: (i) Correct Percentage (the proportion of correct responses); (ii) Omission Rates (the frequency of omission during the sample or choice stage); (iii) Latency to Sample (LS, the time taken from the presentation of the sample lever to the lever press);

(iv) Latency to Choice (LC, the time taken from the presentation of choice lever to the lever press); and (v) Nose Pokes During Delay (the number of nose pokes made during the delay period). Each delay was analyzed individually for correct percentage, omission rates, LC, and nose pokes, while LS was examined across all delays due to the unpredictable duration of the intervals.

The recorded behavioral measures were analyzed using SDT methods [53,54,77]. In this context, a "Hit" was defined as a correct press on the left lever, whereas incorrect presses on the left lever were classified as "false alarms". Accuracy indices, including A' and the SI, along with perceptual/response bias indices, such as B' and the RI, were calculated based on the probabilities of "hit" and "false alarm." In our two-choice task,

$$\mathrm{h} = \mathrm{P(hit)} = \frac{\text{correct left presses}}{\text{correct left presses} + \text{incorrect right presses}}$$

$$\mathrm{f} = \mathrm{P(false\ alarm)} = \frac{\text{incorrect left presses}}{\text{incorrect left presses} + \text{correct right presses}}$$

$$\mathrm{A'} = 0.5 + \frac{(\mathrm{h}-\mathrm{f}) + (\mathrm{h}-\mathrm{f})^2}{4 \times \mathrm{h} \times (1-\mathrm{f})}$$

$$\mathrm{SI} = \frac{(\mathrm{h}-\mathrm{f})}{2 \times (\mathrm{h}+\mathrm{f}) - (\mathrm{h}+\mathrm{f})^2}$$

$$\mathrm{B'} = \mathrm{ABS}\frac{(\mathrm{h}-\mathrm{h}^2) - (\mathrm{f}-\mathrm{f}^2)}{(\mathrm{h}-\mathrm{h}^2) + (\mathrm{f}-\mathrm{f}^2)}$$

$$\mathrm{RI} = \mathrm{ABS}\frac{(\mathrm{h}+\mathrm{f}-1)}{1-(\mathrm{f}-\mathrm{h})^2}$$

SI is a quantitative measure of an animal's ability to distinguish between the presence and absence of a specific target stimulus—that is, to discriminate "signal" from "noise" [54,80]. In the context of the delayed-NMTP task, the SI specifically assesses the animal's ability to discriminate between the correct (novel) and incorrect (familiar) positions. It reflects the accuracy or discriminability of the subject in distinguishing a "signal" (novel position; the correct choice) from "noise" (familiar position; incorrect choice), independent of any systematic response bias.

RI quantifies the subject's general tendency or preference toward making one type of response over another, regardless of actual stimulus presence [54,80]. It measures whether there is a systematic preference for a certain lever, side, or response ("strategy" or "policy") that may reflect motivation, habit, or motoric factors rather than mnemonic discrimination accuracy.

Pharmacological interventions

The D_1R antagonist SCH 39,166 was administered intraperitoneally at a dose of 0.4 mg/kg [81], and the D_2R antagonist Sulpiride was administered at 8 mg/kg [82,83]. Both drugs were administered 15 min prior to WM training.

Chemogenetic activation of DMS D_1R- or D_2R-neurons

To selectively express the Gq-mutant human M3 muscarinic receptor (hM3Dq) in D_1R- or D_2R-neurons, the double-inverted orientation (DIO) strategy was employed [84]. AAV5-EF1a-DIO-hM3Dq-mCherry (300 nL) or

AAV5-EF1a-DIO-mCherry (300 nL) was bilaterally injected into the DMS (AP: +0.98 mm; ML: ±1.20 mm; DV: −2.50 mm) of Drd1a-Cre mice to target D_1R-neurons. Similarly, equivalent injections were performed in the DMS of Adora2a-Cre mice for targeted expression in D_2R-neurons. Mice were allowed a three-week recovery period before undergoing behavioral training. Clozapine-n-oxide (CNO, 1 mg/kg) was administered intraperitoneally (i.p.) 30 min prior to WM training.

Stereotaxic AAV injection, optic fiber implantation

To achieve selective expression of ChR2/ArchT in D_1R- or D_2R-neurons, Cre-dependent $AAV_{2/9}$-EF1a-DIO-ChR2/ArchT was injected into Drd1-Cre or Adora2a-Cre mice. Mice were anesthetized with chloral hydrate (360 mg/kg, i.p.), then head-fixed in a stereotaxic apparatus (David Kopf Instruments) for bilateral injections into the DMS (AP: +0.98 mm; ML: ±1.20 mm; DV: −2.50 mm). Optic fibers were implanted 0.3 mm above the virus injection site. Following a three-week recovery period, mice underwent behavioral training.

To target dopaminergic neurons in the VTA and SNc, "ArchT-mCherry" AAVs driven by the mTH promoter ($AAV_{2/9}$-mTH-ArchT-mCherry) were used. These AAVs were generated by BrainVTA (Wuhan, China) Co., , according to a previous study [60]. The mTH promoter was based on the 2.5-kb region of a published rat Th promoter [61] and was directly cloned from mouse genomic DNA.

Immunohistochemistry

Brain tissues collected 90-min post-light stimulation were analyzed for c-Fos induction. Mice were anesthetized, fixed, and dehydrated. Coronal sections (30 μm) were blocked in a solution of 3% normal donkey serum/0.25% TritonX-100 in PBS for 1h at room temperature, incubated overnight with primary antibodies, and subsequently with secondary antibodies. The sections were washed, mounted, and imaged using a ZEISS confocal microscope. Quantification of c-Fos^+ nuclei were performed using Image J. The primary antibodies used included anti-c-Fos (EMD Millipore, ABE457), anti-TH (Abcam, ab112), and anti-mCherry (Abcam, ab205402).

Statistical analysis

WM behavioral data were analyzed using a repeated measures two-way ANOVA, with training time as the within-subjects effect and the optogenetic or pharmacogenetic manipulations as the between-subjects effect, followed by Bonferroni's post-hoc analysis. Quantitative c-Fos data were evaluated using Independent-Samples *t*-tests.

Supporting information

S1 Fig. Distinct c-Fos activation patterns following optogenetic manipulations of D_2R- or D_1R-neurons. A ArchT inhibition of D_2R-neurons showed that most c-Fos^+ cells did not co-localize with the virus as indicated by the white arrows. **B** ChR2 activation of D_2R-neurons showed that most Fos^+ cells co-localized with the virus as indicated by the white arrows. **C** ArchT inhibition of D_1R-neurons showed that most Fos^+ cells did not co-localize with the virus as indicated by the white arrows. **D** ChR2 activation of D_1R-neurons showed that most Fos^+ cells co-localized with the virus as indicated by the white arrows. Scale bar: 50 μm.
(TIF)

S2 Fig. Effects of optogenetic manipulations of DMS D_2R-neurons on the locomotor activity. A Optogenetic inhibition of DMS D_2R-neurons for 5 min did not significantly alter the distance traveled in the open field test (RM two-way ANOVA, $P > 0.05$; GFP, $n = 6$, ArchT, $n = 7$). **B** Optogenetic activation of DMS D_2R-neurons did not significantly impact locomotion (mCherry, $n = 10$, ChR2, $n = 7$). The data underlying panels A and B can be found in S1 Data.
(TIF)

S3 Fig. Chemogenetic activation of DMS D_2R-neurons significantly impaired WM performance under low cognitive load. A Schematic representation of virus injections of DIO-hM3Dq-mCherry or DIO-mCherry in DMS of Adora2a-Cre (+) mice. **B** Representative images showing hM3Dq expression (red), DAPI (blue), and c-Fos induction in DMS (left, gray), GPe (right top), and SNR (right bottom). Scale bar, 100 μm. **C** Following i.p injection of 1 mg/kg CNO to activate DMS D_2R-neurons, WM performance across sessions was significantly impaired under the 10 s delay condition (RM two-way ANOVA, ## $P<0.01$; Bonferroni's post-hoc comparisons, Day 5 and 6, ** $P<0.01$; mCherry, $n=10$, hM3Dq, $n=13$). **D** The success rate averaged over 6 days was significantly lower following CNO administration under the 10 s delay condition (Independent-Sample *T* test, ** $P<0.01$). The data underlying panel D can be found in S1 Data. Data are represented as mean ± SEM.
(TIF)

S4 Fig. Effects of optogenetic manipulations of D_1R-neurons on locomotor activity. A Optogenetic inhibition of DMS D_1R-neurons for 5 min resulted in a significant reduction in the distance traveled during the open field test (RM two-way ANOVA, * $P<0.05$; GFP, n = 8, ArchT, $n=7$). **B** Optogenetic activation of DMS D_1R-neurons through ChR2 did not significantly affect locomotor activity (mCherry, $n=7$, ChR2, $n=7$). The data underlying panels A and B can be found in S1 Data. Data are represented as mean ± SEM.
(TIF)

S5 Fig. Chemogenetic activation of DMS D_1R-neurons had no significant impact on WM performance under low cognitive load. A Schematic representation of virus injection of DIO-hM3Dq-mCherry in DMS of Drd1-Cre (+) or Drd1-Cre (−) mice. **B** Representative image (left) depicting hM3Dq expression (red), DAPI (blue), and c-Fos induction in DMS (left, gray). Fibers project to GPi (right top) and SNR (right bottom), but no increase in c-Fos expression was detected. Scale bar, 100 μm. **C** Following i.p injection of CNO to activate DMS D_1R-neurons, WM performance across sessions showed no significant effects under low cognitive load (RM two-way ANOVA, $P>0.05$; D1Cre (−), $n=6$, D1Cre (+), $n=6$). **D** The average success rate over 6 days indicated no significant difference (Independent-Sample *T* test, ns $P>0.05$). The data underlying panel D can be found in S1 Data. Data are represented as mean ± SEM.
(TIF)

S6 Fig. Optogenetic inhibition of D_2R-, D_1R-neurons didn't affect motivational and motor states in the operant DNMTP task. A Percentages of correct responses during the NMTP learning stage of the adora2a-Cre mice. **B** Percentages of correct responses during the delayed-NMTP stage of the adora2a-Cre mice demonstrated delay-dependent decline. **C–E** During the "sample" phase, photoinhibition of DMS D_2R-neurons didn't significantly impact LS (**C**), LC (**D**), but increased the number of nose pokes during the delay period (**E,** RM 2-way ANOVA, main effect, $F_{1, 14}=5.533$, #$p<0.05$; interaction, $F_{2, 27}=2.920$, $p>0.05$; Fisher's LSD post-hoc comparisons, Delay 10s, * $p<0.05$). **F–H** During the "delay" phase, photoinhibition of DMS D_2R-neurons didn't significantly affect LS (**F**), LC (**G**), and nose pokes during the delay period (**H**). **I–K** During the "choice" phase, photoinhibition of DMS D_2R-neurons didn't impact LS (**I**), and nose pokes during the delay period (**K**). **J** Photoinhibition of DMS D_2R-neurons during the "choice" phase extended the LC under 10 s delay (RM 2-way ANOVA, main effect, $F_{1, 20}=3.270$, $p>0.05$; interaction, $F_{2, 34}=3.344$, $p<0.05$; Fisher's LSD post-hoc comparisons, Delay 10s, * $p<0.05$). **L** Percentages of correct responses during the NMTP learning stage of the Drd1-Cre mice. **M** Percentages of correct responses during the Delayed-NMTP stage of the Drd1-Cre mice, demonstrating a delay-dependent decline. **N–P** During the "sample" phase, photoinhibition of DMS D_1R-neurons had no significant effects on LS (**N**), LC (**O**), or the number of nose pokes (**P**). **Q–S** During the "delay" phase, photoinhibition of DMS D_1R-neurons didn't affect LS (**Q**), LC (**R**), or the number of nose pokes (**S**). **T–V** During the "choice" phase, photoinhibition of DMS D_1R-neurons didn't impact LS (**T**), LC (**U**), or the number of nose pokes (**V**). Sample size of adora2a-Cre mice: GFP, $n=8$, ArchT, $n=9$; of Drd1-Cre mice: $n=9$ for both ArchT(+) and ArchT(−). The data underlying panels C, F, I, N, Q and T can be found in S1 Data. Data are represented as mean ± SEM.
(TIF)

S7 Fig. Colocalization of ArchT-mCherry expression with TH⁺ dopaminergic neurons in the VTA/SNc. A Representative immunohistochemical images of ArchT-mCherry in the VTA (red) and their overlap with TH⁺ dopaminergic neurons (cyan). Scale bar: 20 μm; **B** Quantification of the percentage of TH⁺/ArchT-mCherry⁺ colocalization in all ArchT-mCherry⁺ neurons in the VTA/SNc across bregma −3.16 mm to −3.64 mm. The data underlying panel B can be found in S1 Data.
(TIF)

S8 Fig. Optogenetic inhibition of VTA/SNc dopaminergic terminals in the DMS reduces calcium activity and dopamine release. A Schematic illustrating viral injections of mTH-ArchT-mCherry and mTH-GCaMP6m into the SNc/VTA and implantation of two optic fibers into the DMS of C57BL/6 mice. **B** Left: Representative images of ArchT expression (red) and GCaMP6m fibers from VTA/SNc (green) in the DMS; Right: Representative images in the SNc/VTA showing ArchT expression (red), GCaMP6m expression (green) and TH staining (magenta). **C** Mean calcium fluorescence intensity ($\Delta F/F$) in the DMS is significantly reduced during 60 s of 560 nm light stimulation of dopaminergic terminals ($n = 5$). **D** Schematic illustrating viral injections of mTH-ArchT-mCherry in the SNc/VTA and AAV-hSyn-DA1h in the DMS, with implantation of two optic fibers in the DMS of C57BL/6 mice. **E** Left: Representative images of ArchT expression (red) and DA1h expression (green) in the DMS; Right: Representative images in the SNc/VTA showing ArchT expression (red) and TH staining (magenta). **F** Mean dopamine fluorescence intensity ($\Delta F/F$) in the DMS is significantly reduced during 60 s of 560 nm light stimulation of dopaminergic terminals ($n = 3$).
(TIF)

S9 Fig. Pharmacological inhibition of dopamine D_1R rescue WM impairment induced by the activation of D_1R-neuron. A Representative image illustrating ChR2 expression in the striatum of Drd1Cre*Ai32 mice, with projections to GPi and SNR. **B** During the 60 s "delay" phase, photoactivation of D_1R-neurons with 470 nm laser led to significant WM impairments (RM two-way ANOVA, main effect, $F_{1, 14} = 20.08$, ###$p < 0.001$, interaction, $F_{6, 84} = 3.513$, $p < 0.001$, Fisher's LSD post-hoc comparisons, Day 4, **$p < 0.01$, Day 5, *$p < 0.05$, Day 6, ***$p < 0.001$, Day 7, ****$p < 0.0001$; $n = 8$ for both groups). **C** Intraperitoneal administration of the D_1R antagonist SCH39166 partially mitigated the WM impairments induced by D_1R-neuron activation (Paired *t* test, *$p < 0.05$). **D** The D_2R antagonist Sulpiride was ineffective in rescuing WM impairment following D_1R-neuron activation. **E** Without interventions, both groups exhibited comparable performance levels. The data underlying panels C, D and E can be found in S1 Data. Data are presented as mean ± SEM.
(TIF)

S1 Data. All individual numerical values corresponding to the data displayed in Figs 1C, 2C, 3C, 4C, 4G, 4J, 4M, 4N, 6E, 6F, 6L, 6M, 6N, S2A, S2B, S3D, S4A, S4B, S5D, S6C, S6F, S6I, S6N, S6Q, S6T, S7B, S9C, S9D and S9E.
(XLSX)

S1 Video. Bilateral activation of D1R⁺ neurons using high intensity laser power caused unilateral rotation in some mice.
(MP4)

Acknowledgments

We thank Weilin Lu, Xiangping Yin, Haiwei Liu, Yuntao Liu, and Yingwen Lu for their generous technical assistance.

Author contributions

Conceptualization: Jiang-fan Chen, Zhihui Li.

Data curation: Xing-jun Chen, Fei Li, Xinyue Zhao, Long Chen, Jin Xue, Zhimo Yao, Zuobin Gan, Xiaoyue Lian, Qin Wang, Zhihui Li.

Formal analysis: Zhimo Yao, Luyao Tong, Qingshan Yan, Linan Qiu, Zhihui Li.

Funding acquisition: Jiang-fan Chen, Zhihui Li.

Investigation: Xing-jun Chen, Fei Li, Xinyue Zhao, Long Chen, Jin Xue, Xiaoyue Lian, Zhenghao Liu, Luyao Tong.

Methodology: Xing-jun Chen, Fei Li, Xinyue Zhao, Long Chen, Jin Xue, Zuobin Gan, Xiaoyue Lian.

Project administration: Jiang-fan Chen, Zhihui Li.

Software: Qingshan Yan, Linan Qiu.

Supervision: Jiang-fan Chen, Zhihui Li.

Validation: Xing-jun Chen.

Visualization: Linan Qiu, Qin Wang.

Writing – original draft: Zhihui Li.

Writing – review & editing: Jiang-fan Chen, Zhihui Li.

References

1. Baddeley A. Working memory. Science. 1992;255(5044):556–9. https://doi.org/10.1126/science.1736359 PMID: 1736359
2. Grady C. The cognitive neuroscience of ageing. Nat Rev Neurosci. 2012;13(7):491–505. https://doi.org/10.1038/nrn3256 PMID: 22714020
3. Lett TA, Voineskos AN, Kennedy JL, Levine B, Daskalakis ZJ. Treating working memory deficits in schizophrenia: a review of the neurobiology. Biol Psychiatry. 2014;75(5):361–70. https://doi.org/10.1016/j.biopsych.2013.07.026 PMID: 24011822
4. Germano C, Kinsella GJ. Working memory and learning in early Alzheimer's disease. Neuropsychol Rev. 2005;15(1):1–10. https://doi.org/10.1007/s11065-005-3583-7 PMID: 15929495
5. Christophel TB, Klink PC, Spitzer B, Roelfsema PR, Haynes J-D. The distributed nature of working memory. Trends Cogn Sci. 2017;21(2):111–24. https://doi.org/10.1016/j.tics.2016.12.007 PMID: 28063661
6. Zhang X, Yan W, Wang W, Fan H, Hou R, Chen Y, et al. Active information maintenance in working memory by a sensory cortex. Elife. 2019;8:e43191. https://doi.org/10.7554/eLife.43191 PMID: 31232695
7. Wang Y, Yin X, Zhang Z, Li J, Zhao W, Guo ZV. A cortico-basal ganglia-thalamo-cortical channel underlying short-term memory. Neuron. 2021;109(21):3486-3499.e7. https://doi.org/10.1016/j.neuron.2021.08.002 PMID: 34469773
8. Guo ZV, Inagaki HK, Daie K, Druckmann S, Gerfen CR, Svoboda K. Maintenance of persistent activity in a frontal thalamocortical loop. Nature. 2017;545(7653):181–6. https://doi.org/10.1038/nature22324 PMID: 28467817
9. Lewis SJG, Dove A, Robbins TW, Barker RA, Owen AM. Striatal contributions to working memory: a functional magnetic resonance imaging study in humans. Eur J Neurosci. 2004;19(3):755–60. https://doi.org/10.1111/j.1460-9568.2004.03108.x PMID: 14984425
10. Levy R, Friedman HR, Davachi L, Goldman-Rakic PS. Differential activation of the caudate nucleus in primates performing spatial and nonspatial working memory tasks. J Neurosci. 1997;17(10):3870–82. https://doi.org/10.1523/JNEUROSCI.17-10-03870.1997 PMID: 9133405
11. Kermadi I, Joseph JP. Activity in the caudate nucleus of monkey during spatial sequencing. J Neurophysiol. 1995;74(3):911–33. https://doi.org/10.1152/jn.1995.74.3.911 PMID: 7500161
12. Akhlaghpour H, Wiskerke J, Choi JY, Taliaferro JP, Au J, Witten IB. Dissociated sequential activity and stimulus encoding in the dorsomedial striatum during spatial working memory. Elife. 2016;5:e19507. https://doi.org/10.7554/eLife.19507 PMID: 27636864
13. McNab F, Klingberg T. Prefrontal cortex and basal ganglia control access to working memory. Nat Neurosci. 2008;11(1):103–7. https://doi.org/10.1038/nn2024 PMID: 18066057
14. Cohen SM. Electrical stimulation of cortical-caudate pairs during delayed successive visual discrimination in monkeys. Acta Neurobiol Exp (Wars). 1972;32(2):211–33. PMID: 4627615
15. Goldman PS, Rosvold HE. The effects of selective caudate lesions in infant and juvenile Rhesus monkeys. Brain Res. 1972;43(1):53–66. https://doi.org/10.1016/0006-8993(72)90274-0 PMID: 4626157
16. Ji J, He D, Jiang Z. Lesions of the basal ganglia and frontal lobe promote differential impairment to working memory and learning ability. Phys Med Rehabil Res. 2017;2(3). https://doi.org/10.15761/pmrr.1000144
17. Chatham CH, Frank MJ, Badre D. Corticostriatal output gating during selection from working memory. Neuron. 2014;81(4):930–42. https://doi.org/10.1016/j.neuron.2014.01.002 PMID: 24559680
18. Chatham CH, Badre D. Multiple gates on working memory. Curr Opin Behav Sci. 2015;1:23–31. https://doi.org/10.1016/j.cobeha.2014.08.001 PMID: 26719851
19. Li Z, Chen X, Wang T, Gao Y, Li F, Chen L, et al. The corticostriatal adenosine A2A receptor controls maintenance and retrieval of spatial working memory. Biol Psychiatry. 2018;83(6):530–41. https://doi.org/10.1016/j.biopsych.2017.07.017 PMID: 28941549.

20. Gerfen CR, Engber TM, Mahan LC, Susel Z, Chase TN, Monsma FJ Jr, et al. D1 and D2 dopamine receptor-regulated gene expression of striatonigral and striatopallidal neurons. Science. 1990;250(4986):1429–32. https://doi.org/10.1126/science.2147780 PMID: 2147780
21. Parent A, Bouchard C, Smith Y. The striatopallidal and striatonigral projections: two distinct fiber systems in primate. Brain Res. 1984;303(2):385–90. https://doi.org/10.1016/0006-8993(84)91224-1 PMID: 6744030
22. Kravitz AV, Tye LD, Kreitzer AC. Distinct roles for direct and indirect pathway striatal neurons in reinforcement. Nat Neurosci. 2012;15(6):816–8. https://doi.org/10.1038/nn.3100 PMID: 22544310
23. Hikida T, Kimura K, Wada N, Funabiki K, Nakanishi S. Distinct roles of synaptic transmission in direct and indirect striatal pathways to reward and aversive behavior. Neuron. 2010;66(6):896–907. https://doi.org/10.1016/j.neuron.2010.05.011 PMID: 20620875
24. Cui G, Jun SB, Jin X, Pham MD, Vogel SS, Lovinger DM, et al. Concurrent activation of striatal direct and indirect pathways during action initiation. Nature. 2013;494(7436):238–42. https://doi.org/10.1038/nature11846 PMID: 23354054
25. Tecuapetla F, Jin X, Lima SQ, Costa RM. Complementary contributions of striatal projection pathways to action initiation and execution. Cell. 2016;166(3):703–15. https://doi.org/10.1016/j.cell.2016.06.032 PMID: 27453468
26. Sheng M-J, Lu D, Shen Z-M, Poo M-M. Emergence of stable striatal D1R and D2R neuronal ensembles with distinct firing sequence during motor learning. Proc Natl Acad Sci U S A. 2019;116(22):11038–47. https://doi.org/10.1073/pnas.1901712116 PMID: 31072930
27. Nonomura S, Nishizawa K, Sakai Y, Kawaguchi Y, Kato S, Uchigashima M, et al. Monitoring and updating of action selection for goal-directed behavior through the striatal direct and indirect pathways. Neuron. 2018;99(6):1302-1314.e5. https://doi.org/10.1016/j.neuron.2018.08.002 PMID: 30146299
28. Vicente AM, Galvão-Ferreira P, Tecuapetla F, Costa RM. Direct and indirect dorsolateral striatum pathways reinforce different action strategies. Curr Biol. 2016;26(7):R267-9. https://doi.org/10.1016/j.cub.2016.02.036 PMID: 27046807
29. O'Hare JK, Ade KK, Sukharnikova T, Van Hooser SD, Palmeri ML, Yin HH, et al. Pathway-specific striatal substrates for habitual behavior. Neuron. 2016;89(3):472–9. https://doi.org/10.1016/j.neuron.2015.12.032 PMID: 26804995
30. Shin JH, Kim D, Jung MW. Differential coding of reward and movement information in the dorsomedial striatal direct and indirect pathways. Nat Commun. 2018;9(1):404. https://doi.org/10.1038/s41467-017-02817-1 PMID: 29374173
31. Alexander GE, Crutcher MD. Functional architecture of basal ganglia circuits: neural substrates of parallel processing. Trends Neurosci. 1990;13(7):266–71. https://doi.org/10.1016/0166-2236(90)90107-l PMID: 1695401
32. DeLong MR. Primate models of movement disorders of basal ganglia origin. Trends Neurosci. 1990;13(7):281–5. https://doi.org/10.1016/0166-2236(90)90110-v PMID: 1695404
33. Bariselli S, Fobbs WC, Creed MC, Kravitz AV. A competitive model for striatal action selection. Brain Res. 2019;1713:70–9. https://doi.org/10.1016/j.brainres.2018.10.009 PMID: 30300636
34. Koziol LF, Budding DE. Procedural Learning. In: Seel NM. Encyclopedia of the sciences of learning. Boston, MA: Springer US. 2012;2694–6.
35. Squire LR, Dede AJO. Conscious and unconscious memory systems. Cold Spring Harb Perspect Biol. 2015;7(3):a021667. https://doi.org/10.1101/cshperspect.a021667 PMID: 25731765
36. Scimeca JM, Badre D. Striatal contributions to declarative memory retrieval. Neuron. 2012;75(3):380–92. https://doi.org/10.1016/j.neuron.2012.07.014 PMID: 22884322
37. Spellman T, Rigotti M, Ahmari SE, Fusi S, Gogos JA, Gordon JA. Hippocampal-prefrontal input supports spatial encoding in working memory. Nature. 2015;522(7556):309–14. https://doi.org/10.1038/nature14445 PMID: 26053122
38. Yamamoto J, Suh J, Takeuchi D, Tonegawa S. Successful execution of working memory linked to synchronized high-frequency gamma oscillations. Cell. 2014;157(4):845–57. https://doi.org/10.1016/j.cell.2014.04.009 PMID: 24768692
39. Bolkan SS, Stujenske JM, Parnaudeau S, Spellman TJ, Rauffenbart C, Abbas AI, et al. Thalamic projections sustain prefrontal activity during working memory maintenance. Nat Neurosci. 2017;20(7):987–96. https://doi.org/10.1038/nn.4568 PMID: 28481349
40. Roy DS, Zhang Y, Aida T, Shen C, Skaggs KM, Hou Y, et al. Anterior thalamic circuits crucial for working memory. Proc Natl Acad Sci U S A. 2022;119(20):e2118712119. https://doi.org/10.1073/pnas.2118712119 PMID: 35537049
41. Vogel P, Hahn J, Duvarci S, Sigurdsson T. Prefrontal pyramidal neurons are critical for all phases of working memory. Cell Rep. 2022;39(2):110659. https://doi.org/10.1016/j.celrep.2022.110659 PMID: 35417688
42. Barrouillet P, Bernardin S, Portrat S, Vergauwe E, Camos V. Time and cognitive load in working memory. J Exp Psychol Learn Mem Cogn. 2007;33(3):570–85. https://doi.org/10.1037/0278-7393.33.3.570 PMID: 17470006
43. Barrouillet P, Bernardin S, Camos V. Time constraints and resource sharing in adults' working memory spans. J Exp Psychol Gen. 2004;133(1):83–100. https://doi.org/10.1037/0096-3445.133.1.83 PMID: 14979753
44. Portrat S, Barrouillet P, Camos V. Time-related decay or interference-based forgetting in working memory?. J Exp Psychol Learn Mem Cogn. 2008;34(6):1561–4. https://doi.org/10.1037/a0013356 PMID: 18980415
45. Barrouillet P, De Paepe A, Langerock N. Time causes forgetting from working memory. Psychon Bull Rev. 2012;19(1):87–92. https://doi.org/10.3758/s13423-011-0192-8 PMID: 22184034
46. Schneegans S, Bays PM. Drift in neural population activity causes working memory to deteriorate over time. J Neurosci. 2018;38(21):4859–69. https://doi.org/10.1523/JNEUROSCI.3440-17.2018 PMID: 29703786

47. Gobin C, Wu L, Schwendt M. Using rat operant delayed match-to-sample task to identify neural substrates recruited with increased working memory load. Learn Mem. 2020;27(11):467–76. https://doi.org/10.1101/lm.052134.120 PMID: 33060284
48. Deacon RMJ, Rawlins JNP. T-maze alternation in the rodent. Nat Protoc. 2006;1(1):7–12. https://doi.org/10.1038/nprot.2006.2 PMID: 17406205
49. Kreitzer AC. Physiology and pharmacology of striatal neurons. Annu Rev Neurosci. 2009;32:127–47. https://doi.org/10.1146/annurev.neuro.051508.135422 PMID: 19400717
50. Tepper JM, Koós T, Wilson CJ. GABAergic microcircuits in the neostriatum. Trends Neurosci. 2004;27(11):662–9. https://doi.org/10.1016/j.tins.2004.08.007 PMID: 15474166
51. Gittis AH, Nelson AB, Thwin MT, Palop JJ, Kreitzer AC. Distinct roles of GABAergic interneurons in the regulation of striatal output pathways. J Neurosci. 2010;30(6):2223–34. https://doi.org/10.1523/JNEUROSCI.4870-09.2010 PMID: 20147549
52. Mestres-Missé A, Turner R, Friederici AD. An anterior-posterior gradient of cognitive control within the dorsomedial striatum. Neuroimage. 2012;62(1):41–7. https://doi.org/10.1016/j.neuroimage.2012.05.021 PMID: 22617829
53. Steckler T. Using signal detection methods for analysis of operant performance in mice. Behav Brain Res. 2001;125(1–2):237–48. https://doi.org/10.1016/s0166-4328(01)00305-9 PMID: 11682115
54. Marston HM. Analysis of cognitive function in animals, the value of SDT. Brain Res Cogn Brain Res. 1996;3(3–4):269–77. https://doi.org/10.1016/0926-6410(96)00012-2 PMID: 8806028
55. Sippy T, Lapray D, Crochet S, Petersen CCH. Cell-type-specific sensorimotor processing in striatal projection neurons during goal-directed behavior. Neuron. 2015;88(2):298–305. https://doi.org/10.1016/j.neuron.2015.08.039 PMID: 26439527
56. Shan Q, Ge M, Christie MJ, Balleine BW. The acquisition of goal-directed actions generates opposing plasticity in direct and indirect pathways in dorsomedial striatum. J Neurosci. 2014;34(28):9196–201. https://doi.org/10.1523/JNEUROSCI.0313-14.2014 PMID: 25009253
57. Seamans JK, Yang CR. The principal features and mechanisms of dopamine modulation in the prefrontal cortex. Prog Neurobiol. 2004;74(1):1–58. https://doi.org/10.1016/j.pneurobio.2004.05.006 PMID: 15381316
58. Gruber AJ, Dayan P, Gutkin BS, Solla SA. Dopamine modulation in the basal ganglia locks the gate to working memory. J Comput Neurosci. 2006;20(2):153–66. https://doi.org/10.1007/s10827-005-5705-x PMID: 16699839
59. Bäckman L, Nyberg L, Soveri A, Johansson J, Andersson M, Dahlin E, et al. Effects of working-memory training on striatal dopamine release. Science. 2011;333(6043):718. https://doi.org/10.1126/science.1204978 PMID: 21817043
60. Chan KY, Jang MJ, Yoo BB, Greenbaum A, Ravi N, Wu W-L, et al. Engineered AAVs for efficient noninvasive gene delivery to the central and peripheral nervous systems. Nat Neurosci. 2017;20(8):1172–9. https://doi.org/10.1038/nn.4593 PMID: 28671695
61. Oh MS, Hong SJ, Huh Y, Kim K-S. Expression of transgenes in midbrain dopamine neurons using the tyrosine hydroxylase promoter. Gene Ther. 2009;16(3):437–40. https://doi.org/10.1038/gt.2008.148 PMID: 18800154
62. Lammel S, Steinberg EE, Földy C, Wall NR, Beier K, Luo L, et al. Diversity of transgenic mouse models for selective targeting of midbrain dopamine neurons. Neuron. 2015;85(2):429–38. https://doi.org/10.1016/j.neuron.2014.12.036 PMID: 25611513
63. Mahn M, Prigge M, Ron S, Levy R, Yizhar O. Biophysical constraints of optogenetic inhibition at presynaptic terminals. Nat Neurosci. 2016;19(4):554–6. https://doi.org/10.1038/nn.4266 PMID: 26950004
64. Bolkan SS, Stone IR, Pinto L, Ashwood ZC, Iravedra Garcia JM, Herman AL, et al. Opponent control of behavior by dorsomedial striatal pathways depends on task demands and internal state. Nat Neurosci. 2022;25(3):345–57. https://doi.org/10.1038/s41593-022-01021-9 PMID: 35260863
65. Pertzov Y, Manohar S, Husain M. Rapid forgetting results from competition over time between items in visual working memory. J Exp Psychol Learn Mem Cogn. 2017;43(4):528–36. https://doi.org/10.1037/xlm0000328 PMID: 27668485
66. Barrouillet P, Bernardin S, Portrat S, Vergauwe E, Camos V. Time and cognitive load in working memory. J Exp Psychol Learn Mem Cogn. 2007;33(3):570–85. https://doi.org/10.1037/0278-7393.33.3.570 PMID: 17470006
67. Burak Y, Fiete IR. Fundamental limits on persistent activity in networks of noisy neurons. Proc Natl Acad Sci U S A. 2012;109(43):17645–50. https://doi.org/10.1073/pnas.1117386109 PMID: 23047704
68. Wimmer K, Nykamp DQ, Constantinidis C, Compte A. Bump attractor dynamics in prefrontal cortex explains behavioral precision in spatial working memory. Nat Neurosci. 2014;17(3):431–9. https://doi.org/10.1038/nn.3645 PMID: 24487232
69. Zhu J, Cheng Q, Chen Y, Fan H, Han Z, Hou R, et al. Transient delay-period activity of agranular insular cortex controls working memory maintenance in learning novel tasks. Neuron. 2020;105(5):934-946.e5. https://doi.org/10.1016/j.neuron.2019.12.008 PMID: 32135091
70. Kellendonk C, Simpson EH, Polan HJ, Malleret G, Vronskaya S, Winiger V, et al. Transient and selective overexpression of dopamine D2 receptors in the striatum causes persistent abnormalities in prefrontal cortex functioning. Neuron. 2006;49(4):603–15. https://doi.org/10.1016/j.neuron.2006.01.023 PMID: 16476668
71. Seeman P, Kapur S. Schizophrenia: more dopamine, more D2 receptors. Proc Natl Acad Sci U S A. 2000;97(14):7673–5. https://doi.org/10.1073/pnas.97.14.7673 PMID: 10884398
72. Cazorla M, Shegda M, Ramesh B, Harrison NL, Kellendonk C. Striatal D2 receptors regulate dendritic morphology of medium spiny neurons via Kir2 channels. J Neurosci. 2012;32(7):2398–409. https://doi.org/10.1523/JNEUROSCI.6056-11.2012 PMID: 22396414

73. Duvarci S, Simpson EH, Schneider G, Kandel ER, Roeper J, Sigurdsson T. Impaired recruitment of dopamine neurons during working memory in mice with striatal D2 receptor overexpression. Nat Commun. 2018;9(1):2822. https://doi.org/10.1038/s41467-018-05214-4 PMID: 30026489

74. Wilhelm M, Sych Y, Fomins A, Alatorre Warren JL, Lewis C, Serratosa Capdevila L, et al. Striatum-projecting prefrontal cortex neurons support working memory maintenance. Nat Commun. 2023;14(1):7016. https://doi.org/10.1038/s41467-023-42777-3 PMID: 37919287

75. Vorhees CV, Williams MT. Assessing spatial learning and memory in rodents. ILAR J. 2014;55(2):310–32. https://doi.org/10.1093/ilar/ilu013 PMID: 25225309

76. Liu D, Gu X, Zhu J, Zhang X, Han Z, Yan W, et al. Medial prefrontal activity during delay period contributes to learning of a working memory task. Science. 2014;346(6208):458–63. https://doi.org/10.1126/science.1256573 PMID: 25342800

77. Estapé N, Steckler T. Effects of cholinergic manipulation on operant delayed non-matching to position performance in two inbred strains of mice. Behav Brain Res. 2001;121(1–2):39–55. https://doi.org/10.1016/s0166-4328(00)00379-x PMID: 11275283

78. Dunnett SB, White A. Striatal grafts alleviate bilateral striatal lesion deficits in operant delayed alternation in the rat. Exp Neurol. 2006;199(2):479–89. https://doi.org/10.1016/j.expneurol.2006.01.013 PMID: 16516889

79. Estapé N, Steckler T. Cholinergic blockade impairs performance in operant DNMTP in two inbred strains of mice. Pharmacol Biochem Behav. 2002;72(1–2):319–34. https://doi.org/10.1016/s0091-3057(01)00747-x PMID: 11900803

80. Steckler T. Using signal detection methods for analysis of operant performance in mice. Behav Brain Res. 2001;125(1–2):237–48. https://doi.org/10.1016/s0166-4328(01)00305-9 PMID: 11682115

81. Katz JL, Kopajtic TA, Myers KA, Mitkus RJ, Chider M. Behavioral effects of cocaine: interactions with D1 dopaminergic antagonists and agonists in mice and squirrel monkeys. J Pharmacol Exp Ther. 1999;291(1):265–79. https://doi.org/10.1016/s0022-3565(24)35097-9 PMID: 10490913

82. Fujiwara H. Comparative studies of sulpiride and classical neuroleptics on induction of catalepsy, locomotor activity, and brain dopamine metabolism in mice. Pharmacol Biochem Behav. 1992;41(2):301–8. https://doi.org/10.1016/0091-3057(92)90102-l PMID: 1349435

83. Zarrindast M-R, Fazli-Tabaei S, Khakpai F. Synergistic effect between quinpirole and L-NAME as well as sulpiride and L-arginine on the modulation of anxiety and memory processes in the 6-OHDA mouse model of Parkinson's disease: an isobologram analysis. Neurobiol Learn Mem. 2021;186:107538. https://doi.org/10.1016/j.nlm.2021.107538 PMID: 34737042

84. Armbruster BN, Li X, Pausch MH, Herlitze S, Roth BL. Evolving the lock to fit the key to create a family of G protein-coupled receptors potently activated by an inert ligand. Proc Natl Acad Sci U S A. 2007;104(12):5163–8. https://doi.org/10.1073/pnas.0700293104 PMID: 17360345